



Calhoun: The NPS Institutional Archive

Theses and Dissertations

Thesis Collection

1969-06

An investigation of oscillations in an adaptive aircraft control system under large input commands.

Wilser, Larry Smith

Monterey, California. Naval Postgraduate School

<http://hdl.handle.net/10945/40133>



Calhoun is a project of the Dudley Knox Library at NPS, furthering the precepts and goals of open government and government transparency. All information contained herein has been approved for release by the NPS Public Affairs Officer.

**Dudley Knox Library / Naval Postgraduate School
411 Dyer Road / 1 University Circle
Monterey, California USA 93943**

<http://www.nps.edu/library>

United States Naval Postgraduate School



THESIS

AN INVESTIGATION OF OSCILLATIONS IN AN ADAPTIVE
AIRCRAFT CONTROL SYSTEM UNDER LARGE INPUT COMMANDS

by

Larry Smith Wisler

June 1969

THESIS
W6636

*This document has been approved for public re-
lease and sale; its distribution is unlimited.*

U.S. Naval Postgraduate School
Monterey, California 93940

An Investigation of Oscillations
In An Adaptive Aircraft Control System
Under Large Input Commands

by

Larry Smith Wisler
Lieutenant (junior grade), United States Navy
B. S., University of Kansas, 1968

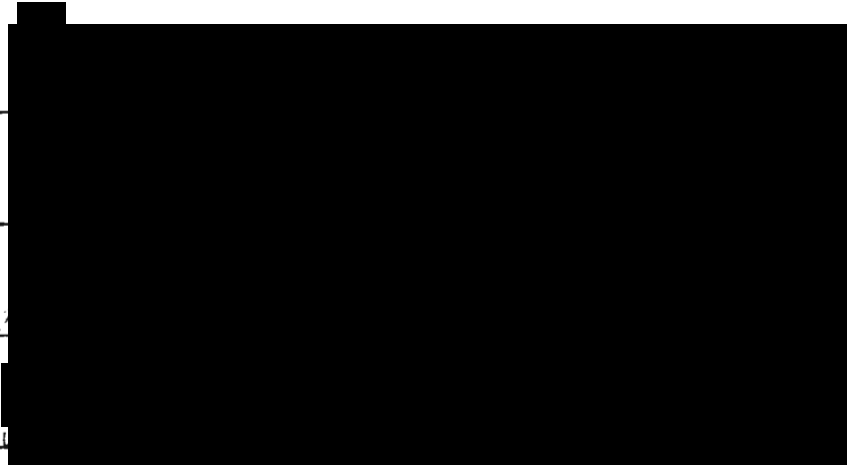
Submitted in partial fulfillment of the
requirements for the degree of

MASTER OF SCIENCE IN AERONAUTICAL ENGINEERING

from the
NAVAL POSTGRADUATE SCHOOL
June 1969

Author

Approved by:



ABSTRACT

An adaptive control scheme for aircraft was studied to find the cause of limit cycles which occurred under large input commands and to find a method for eliminating the oscillations. The complexity of the system equations dictated that all analytical studies be performed on simplified versions of the adaptive control scheme. After exhaustive analysis of the cause of limit cycles in the simplified systems and an investigation of possible fixes for this problem, it was decided that the oscillations were an inherent feature of the control scheme resulting from the servo and actuator lags.

A second adaptive control scheme was thus developed which obtained more feedback information downstream of the aircraft actuator and series servo. A comparison of the two adaptive systems was made under similar flight conditions for the F-4 aircraft and the modified adaptive controller was shown to be practical and free of limit cycle oscillations by analog simulation.

TABLE OF CONTENTS

I.	INTRODUCTION -----	13
II.	THE NONVARYING-C* ADAPTIVE CONTROLLER -----	15
III.	ANALOG SIMULATION FOR THE C*-CONTROL SYSTEM -----	23
IV.	STUDY OF LIMIT CYCLES AND POSSIBLE FIXES -----	49
V.	MODIFICATION OF THE SIMPLIFIED Γ_δ C-CONTROLLER -----	57
VI.	THE MODIFIED NONVARYING-C* ADAPTIVE CONTROLLER -----	65
VII.	ANALOG STUDY OF TWO NONVARYING-C* ADAPTIVE CONTROL SYSTEMS --	69
VIII.	CONCLUSIONS AND RECOMMENDATIONS -----	78
	BIBLIOGRAPHY -----	81
	INITIAL DISTRIBUTION LIST -----	82
	FORM DD 1473 -----	83

LIST OF TABLES

I. Aircraft and Controller Parameters, F-4 Aircraft -----	47
II. Ideal Values of Variable Gains, Original and Modified Controllers -----	48

LIST OF FIGURES

1. Block Diagram for Nonvarying-C* Control System -----	17
2. Block Diagram for Simplified $\Gamma_\delta C$ -Control System -----	21
3. Second Order Servo Model -----	24
4. Analog Trace for $\Gamma_\delta C$ -System, without Servo -----	25
5. Analog Trace for $\Gamma_\delta C$ -System, Neutral Stability Oscillations ---	26
6. Analog Diagram for $\Gamma_\delta C$ -System -----	27
7. Analog Trace for $\Gamma_\delta C$ -System, Limit Cycle Oscillations (Relay) -	28
8. Analog Trace for $\Gamma_\delta C$ -System, Limit Cycle Oscillations (Relay) -	29
9. Block Diagram for Simplified $\Gamma_q \dot{\theta}$ -Control System -----	31
10. Analog Trace for $\Gamma_q \dot{\theta}$ -System, without Servo -----	33
11. Analog Trace for $\Gamma_q \dot{\theta}$ -System, Neutral Stability Oscillations ---	34
12. Analog Diagram for $\Gamma_q \dot{\theta}$ -System -----	35
13. Analog Trace for $\Gamma_q \dot{\theta}$ -System, Limit Cycle Oscillations (Relay) -	36
14. Analog Diagram for Nonvarying-C* Control System -----	37,38
15. Analog Trace for C*-Controller, Free Aircraft without Actuator	39
16. Analog Trace for C*-Controller, Free Aircraft with Actuator ---	40
17. Analog Trace for C*-Controller, without Actuator -----	41
18. Analog Trace for C*-Controller, without Actuator -----	42
19. Analog Trace for C*-Controller, with Actuator -----	43
20. Analog Trace for C*-Controller, with Actuator -----	44
21. Analog Trace for C*-Controller, with Actuator and Servo -----	46
22. Block Diagram for Perturbed $\Gamma_\delta C$ -System -----	52
23. Bode Plot for $\Gamma_\delta C$ -System -----	53
24. Analog Trace for $\Gamma_q \dot{\theta}$ -System, Eliminate Limit Cycles with Deadband Increase $\epsilon_0 = .08$ -----	55

LIST OF FIGURES (continued)

25. Block Diagram for Modified $\Gamma_\delta C$ -System -----	58
26. Block Diagram for Perturbed Modified $\Gamma_\delta C$ -System -----	62
27. Analog Trace for Modified $\Gamma_\delta C$ -System, No Limit Cycles -----	63
28. Block Diagram for Modified Nonvarying- C^* Control System -----	67
29. Analog Diagram for Modified Nonvarying- C^* Control System --	70,71,72
30. Analog Trace for Modified C^* -Controller, without Servo -----	73
31. Analog Trace for Modified C^* -Controller, Flight Condition Mach 2.0, 50,000 feet -----	75
32. Analog Trace for Modified C^* -Controller, Flight Condition Mach 0.2, Sea Level -----	76
33. Analog Trace for Modified C^* -Controller, Flight Condition Mach 0.9, Sea Level -----	77

LIST OF SYMBOLS

Symbol	Definition
A	Amplitude of Limit Cycle Oscillations
C	Input Command
C*	Boeing Performance Criterion
f	Control Function
K _q	Positive Constant Gain
K _n	Positive Constant Gain
K _δ	Positive Constant Gain
l _p	Distance the Pilot is Forward of the Center of Gravity
M _α	Pitching Moment Change due to Angle of Attack Change $\frac{1}{I_y} \frac{\partial M}{\partial \alpha}$
M _q	Pitching Moment Change due to Pitch Rate Change $\frac{1}{I_y} \frac{\partial M}{\partial q}$
M _δ	Pitching Moment Change due to Elevator Angle Change $\frac{1}{I_y} \frac{\partial M}{\partial \delta}$
M _{α̇}	Pitching Moment Change due to Attack Angle Rate Change $\frac{1}{I_y} \frac{\partial M}{\partial \dot{\alpha}}$
n	Normal Acceleration
S	Laplacian Operator
t	Time
U ₀	Unperturbed Velocity
V _c	Cross-over Velocity ≈ 400 feet/sec.
Z _α	Side Force Change due to Angle of Attack Change $\frac{1}{m} \frac{\partial Z}{\partial \alpha}$
Z _δ	Side Force Change due to Elevator Angle Change $\frac{1}{m} \frac{\partial Z}{\partial \delta}$

LIST OF SYMBOLS (continued)

Greek Symbol	Definition
α	Angle of Attack
$\dot{\alpha}$	Attack Angle Rate
β_q	$-\frac{V_c}{\ell_p}$
β_δ	$-\frac{k}{\ell_p}$
β_n	$-\frac{1}{\ell_p}$
$\bar{\beta}_q$	$M_\delta - \frac{Z_\delta M_\alpha}{Z_\alpha}$
$\bar{\beta}_n$	$M_q + M_{\dot{\alpha}}$
$\bar{\beta}_\delta$	$-\frac{M_\alpha}{Z_\alpha} - \frac{M_{\dot{\alpha}}}{U_0}$
γ	Small Perturbation Term
Γ_q	Variable Gain
Γ_n	Variable Gain
Γ_δ	Variable Gain
δ_e	Elevator Deflection Angle
ϵ	Error
ζ	Damping Ratio
$\dot{\theta}$	Pitch Rate
$\ddot{\theta}$	Pitch Acceleration
Π	Product Symbol
\sum	Summation Symbol
ω	Frequency of Second Order Servo
Ω	Frequency of Limit Cycle Oscillations

ACKNOWLEDGEMENTS

The author wishes to express his appreciation to Dr. E. R. Rang for his invaluable assistance and advice while pursuing this project and to Mr. Robert Limes for his assistance on the hybrid computer. The author is especially indebted to his wife, Mary, for her patience and understanding during the preparation of this thesis.

I. INTRODUCTION

During the past few years, a new control concept has developed in the field of automatic control. The concept of self-adaptive control made possible the capability of inherently satisfying desired system performance criteria in the presence of a changing environment. An adaptive control system can change its parameters through an internal process of measurement and evaluation of dynamic performance.

Although self-adaptive control systems were found to be successful in most respects, they do exhibit undesirable characteristics. Controllers which detect limit cycles, either intentionally, as in the Honeywell control system for the X-15, or unintentionally, as in the General Electric control system for the F-111, can be upset by air turbulence unless special precautions are taken which reduce the effectiveness and increase the complexity of the system. One such control system, a nonvarying- C^* adaptive control scheme for aircraft was proposed by Rang, Reference 1. The desired system performance criterion, the Boeing C^* -Criterion, specifies that the time response of the quantity C^* fall within a prescribed envelope, for all speeds and altitudes, thus the name nonvarying- C^* controller. This control system, as other similar adaptive systems, exhibits undesirable limit cycles under high input commands. An analog study was conducted in an effort to find the cause of these limit cycles and provide a method or methods of eliminating the oscillations. The study was accomplished at the Naval Postgraduate School Hybrid Computer Facility, Monterey, California, during the period November, 1968, through June, 1969.

The hybrid computer facility consists of a high speed digital computer model 9300 manufactured by Scientific Data Systems of Santa Monica, California, and an electronic analog computer model CI 5000 manufactured by COMCOR, Ind., of Anaheim, California, together with extensive software. Various displays are available including a X-Y recorder, a six channel recorder, and two general purpose high performance input/output consoles which have cathode ray tubes and light pens as well as keyboards.

The 9300-Computer is a high speed, general purpose digital computer. The various input/output devices include: teletype, paper tape, magnetic tape, light pen, and analog interface. The system is operated directly by the user and utilizes FORTRAN IV language.

The CI 5000 is a large scale, general purpose electronic analog/hybrid computer. It is equipped with summers, integrators, inverters, diode function generators, electronic resolvers, quarter square multipliers, D/A converters, A/D trunks, comparaters, relays, manual and servo potentiometers.

The adaptive control system simulation used only the analog computer; however, for future study on such problems the hybrid capability of the computer could be utilized by programming the digital machine to automatically set the potentiometers for each new flight condition or for different aircraft under study.

II. THE NONVARYING-C* ADAPTIVE CONTROLLER

The original nonvarying-C* adaptive controller was developed beginning with the short period aircraft perturbation equations of motion.

$$\ddot{\theta} = M_q \dot{\theta} + M_\alpha \alpha + M_{\dot{\alpha}} \dot{\alpha} + M_\delta \delta_e$$

$$n = U_0 (\dot{\theta} - \dot{\alpha}) = -Z_\alpha \alpha - Z_\delta \delta_e$$

where the aircraft coefficients M_q , M_α , $M_{\dot{\alpha}}$, M_δ , Z_α , and Z_δ are constants representative of a specific flight condition. It is desirable to provide uniform response in a changing environment without using measurements of altitude, dynamic pressure, or angle of attack. Further, angle of attack is difficult to measure and contributions to angle of attack provided by gusts are difficult to distinguish from the motion of the aircraft; therefore, angle of attack is eliminated from the equations.

$$\ddot{\theta} = M_q \dot{\theta} + M_\alpha \left[-\frac{n}{Z_\alpha} - \frac{Z_\delta}{Z_\alpha} \delta_e \right] + M_{\dot{\alpha}} \left[\dot{\theta} - \frac{n}{U_0} \right] + M_\delta \delta_e$$

$$\dot{n} = -Z_\alpha \left[\dot{\theta} - \frac{n}{U_0} \right] - Z_\delta \dot{\delta}_e$$

If the following substitutions are made,

$$\bar{\beta}_\delta = M_\delta - \frac{Z_\delta M_\alpha}{Z_\alpha}$$

$$\bar{\beta}_q = M_q + M_{\dot{\alpha}}$$

$$\bar{\beta}_n = -\frac{M_\alpha}{Z_\alpha} - \frac{M_{\dot{\alpha}}}{U_0}$$

the fundamental equation in the study is derived as

$$\ddot{\theta} = \bar{\beta}_q \dot{\theta} + \bar{\beta}_n n + \bar{\beta}_\delta \delta_e$$

The desired system performance criterion, the Boeing C* criterion, is the sum of the normal force at the pilot's seat, $n + \ell_p \ddot{\theta}$, and a constant

multiple of pitch rate, $V_c \dot{\theta}$, thus

$$C^* = n + \ell_p \ddot{\theta} + V_c \dot{\theta}.$$

The normal acceleration term dominates at high speeds and the pitch rate term dominates at low speeds. If C^* is required to be a constant multiple of the input command, it may be seen that the C^* -criterion is in exactly the same form as the fundamental equation,

$$\ddot{\theta} = -\frac{V_c}{\ell_p} \dot{\theta} - \frac{1}{\ell_p} n - \frac{k}{\ell_p} C$$

$$\ddot{\theta} = \bar{\beta}_q \dot{\theta} + \bar{\beta}_n n + \bar{\beta}_\delta \delta_e$$

where coefficients $\bar{\beta}_q$, $\bar{\beta}_n$, and $\bar{\beta}_\delta$ are negative for all flight conditions.

Now set

$$\beta_q = -\frac{V_c}{\ell_p}$$

$$\beta_n = -\frac{1}{\ell_p}$$

$$\beta_\delta = -\frac{k}{\ell_p}$$

and the C^* -criterion becomes

$$\ddot{\theta} = \beta_q \dot{\theta} + \beta_n n + \beta_\delta C.$$

If a control function could now be found whose gains vary so that for each different flight condition the control system behaved as if the fundamental aircraft equation $\ddot{\theta} - \bar{\beta}_q \dot{\theta} - \bar{\beta}_n n - \bar{\beta}_\delta \delta_e = 0$ were replaced by the system performance criterion $\ddot{\theta} - \beta_q \dot{\theta} - \beta_n n - \beta_\delta C = 0$, then the system would be adaptive. If we neglect the actuator, servo, and actuator model in the analysis for the present, this control function may be taken as

$$f = \Gamma_q \dot{\theta} + \Gamma_n n + \Gamma_\delta C$$

and $\delta_e = C + f.$

The configuration is shown in Figure 1.

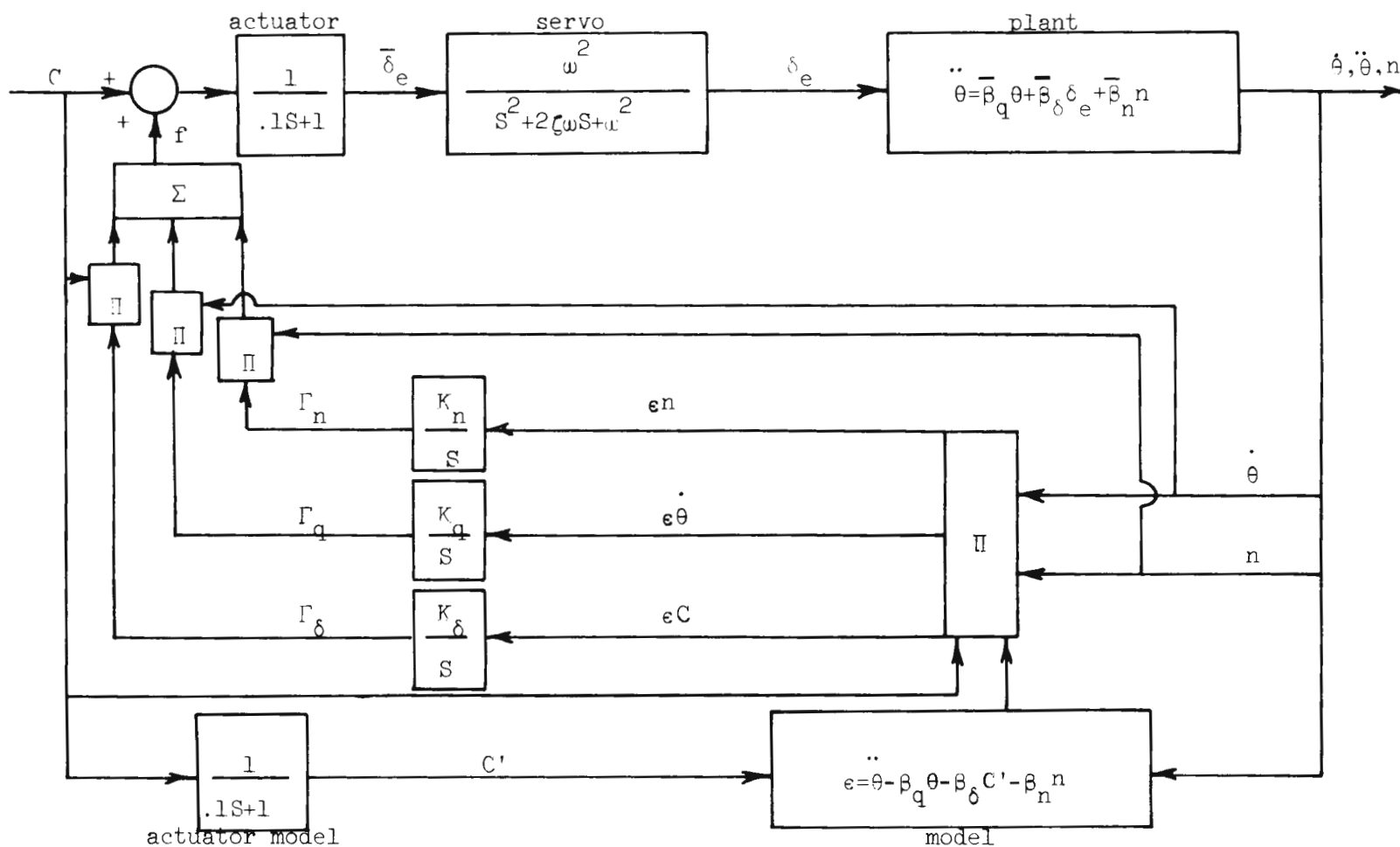


FIGURE 1. BLOCK DIAGRAM FOR NONVARYING- C^* CONTROL SYSTEM

An error signal detects the amount the system criterion deviates from zero.

$$\epsilon = \ddot{\theta} - \beta_q \dot{\theta} - \beta_n n - \beta_\delta C.$$

Substituting the fundamental aircraft equation and the control function yields the following error relationship upon which the derivation of the variable gains is based:

$$\begin{aligned} \epsilon = & \left[\bar{\beta}_q + \bar{\beta}_\delta \Gamma_q - \beta_q \right] \dot{\theta} \\ & + \left[\bar{\beta}_n + \bar{\beta}_\delta \Gamma_n - \beta_n \right] n \\ & + \left[\bar{\beta}_\delta + \bar{\beta}_\delta \Gamma_\delta - \beta_\delta \right] C. \end{aligned}$$

Thus the following ideal values of the variable gains will yield zero error:

$$\Gamma_q^* = \frac{\beta_q - \bar{\beta}_q}{\bar{\beta}_\delta}; \quad \Gamma_n^* = \frac{\beta_n - \bar{\beta}_n}{\bar{\beta}_\delta}; \quad \Gamma_\delta^* = \frac{\beta_\delta - \bar{\beta}_\delta}{\bar{\beta}_\delta}.$$

It is necessary to derive equations for these gains which will drive the system error to zero. Shipley, Reference 2, suggests a gradient technique which has become standard in such derivations. The calculations are:

$$2v = \frac{1}{K_q} \left[\bar{\beta}_q + \bar{\beta}_\delta \Gamma_q - \beta_q \right]^2 + \frac{1}{K_n} \left[\bar{\beta}_n + \bar{\beta}_\delta \Gamma_n - \beta_n \right]^2 + \frac{1}{K_\delta} \left[\bar{\beta}_\delta + \bar{\beta}_\delta \Gamma_\delta - \beta_\delta \right]^2$$

$$\begin{aligned} \frac{dv}{dt} = & \left\{ \frac{1}{K_q} \left[\bar{\beta}_q + \bar{\beta}_\delta \Gamma_q - \beta_q \right] \frac{d\Gamma_q}{dt} \right. \\ & + \frac{1}{K_n} \left[\bar{\beta}_n + \bar{\beta}_\delta \Gamma_n - \beta_n \right] \frac{d\Gamma_n}{dt} \\ & \left. + \frac{1}{K_\delta} \left[\bar{\beta}_\delta + \bar{\beta}_\delta \Gamma_\delta - \beta_\delta \right] \frac{d\Gamma_\delta}{dt} \right\} \bar{\beta}_\delta. \end{aligned}$$

If the variable gains are chosen to make the gradient $dv/dt < 0$, then as time proceeds, v and hence ϵ approach zero.

Choose: $\frac{d\Gamma_q}{dt} = K_q \dot{\theta} G$

$$\frac{d\Gamma_n}{dt} = K_n n G$$

$$\frac{d\Gamma_\delta}{dt} = K_\delta C G$$

Thus $\frac{dv}{dt} = \bar{\beta}_\delta \epsilon G$.

Observing that $\bar{\beta}_\delta$ is always negative and setting G equal to ϵ or $\text{sgn} \epsilon$, the gradient dv/dt is consistently negative. Thus at each flight condition, the error will approach zero and the variable gains will approach their ideal values.

Due to the complex nature of the equations of this adaptive control scheme, simplified versions of the scheme were developed which could be exactly and completely studied analytically. As a first cut, the simplest system was considered. The fundamental equation was reduced to the following:

$$\ddot{\theta} = \bar{\beta}_\delta \delta_e$$

The entire system should now behave like the model or criterion, $\ddot{\theta} = \beta_\delta C$. The error equation reduces to $\epsilon = \ddot{\theta} - \beta_\delta C$ and the control function reduces to $f = \Gamma_\delta C$. Since $\delta_e = C + f$ (neglecting servo), the relationship for the ideal value of the variable gain, Γ_δ , can be calculated,

$$\epsilon = \ddot{\theta} - \beta_\delta C$$

$$\epsilon = \bar{\beta}_\delta \delta_e - \beta_\delta C$$

$$\epsilon = \bar{\beta}_\delta (1 + \Gamma_\delta) C - \beta_\delta C$$

$$\therefore \Gamma_\delta^* = \frac{\beta_\delta - \bar{\beta}_\delta}{\bar{\beta}_\delta} \text{ for } \epsilon \equiv 0$$

as was the case for the complete system.

Therefore, the controller is stable if $2\zeta\omega > -K_\delta C_0^2 \bar{\beta}_\delta$ ($\bar{\beta}_\delta < 0$).

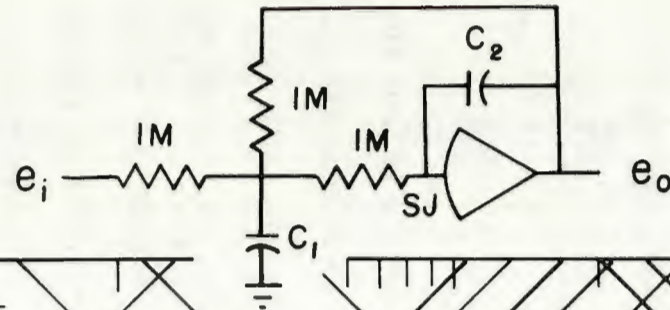
Therefore, for a given servo, ζ and ω are fixed and the system may be driven unstable by sufficiently increasing K_δ or C_0 . Since C_0 is a squared term, the system stability is largely determined by this quantity. It is now obvious why the limit cycles are most predominant under large input commands.

III. ANALOG SIMULATION FOR THE C*-CONTROL SYSTEM

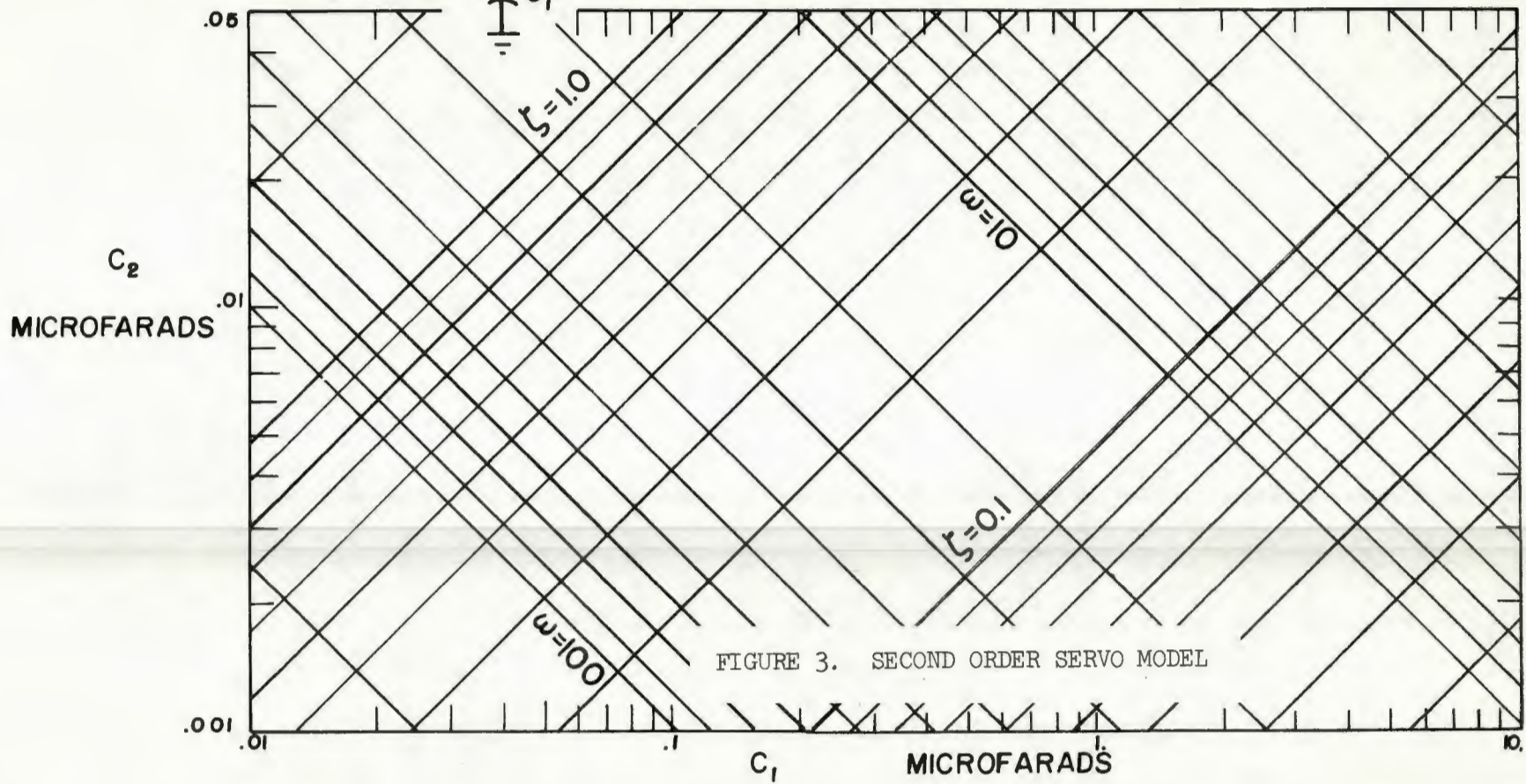
The CI-5000 analog computer was used to simulate the simplified controller. The second order servo was modeled by the circuit shown in Figure 3, where C_1 and C_2 were decade capacitor boxes. The values of ζ and ω for the servo could be provided by appropriately setting C_1 and C_2 from the log-log graph in Figure 3. The simplified controller was first operated with $G=\epsilon$, which provided a linear system. The system was run without the servo, C_1 and C_2 equal zero, and the convergence of the gain to its ideal value was verified, Figure 4. The decade capacitor boxes were then set to give neutral stability, or a simulated limit cycle, Figure 5. The controller was altered by setting $G = \text{sgn}\epsilon$ and replacing a multiplier by a relay on the analog computer, see Figure 6. With the same settings on the decade capacitor boxes or any more unstable settings, this controller would exhibit limit cycles as shown in Figures 7 and 8, instead of a divergent instability.

A second simplified version of the nonvarying-C* controller was then studied to note the increase in complexity toward the full adaptive system and to verify the existence of limit cycles in an unstable non-linear system. The equations which describe this system now include the $\dot{\theta}$ terms, but assume $\bar{\beta}_\delta = \beta_\delta$. The equations are more complex and include more of the terms of the complete controller, therefore yielding results which better approximate the complete control system. The set of equations are:

$$\begin{aligned}\ddot{\theta} &= \bar{\beta}_q \dot{\theta} + \beta_\delta \delta_e \\ \epsilon &= \ddot{\theta} - \beta_q \dot{\theta} - \beta_\delta C \\ \bar{\delta}_e &= C + f = C + \Gamma_q \dot{\theta}\end{aligned}$$



$$\frac{e_o}{e_i} = \frac{-\omega^2}{s^2 + 2\zeta\omega s + \omega^2}$$



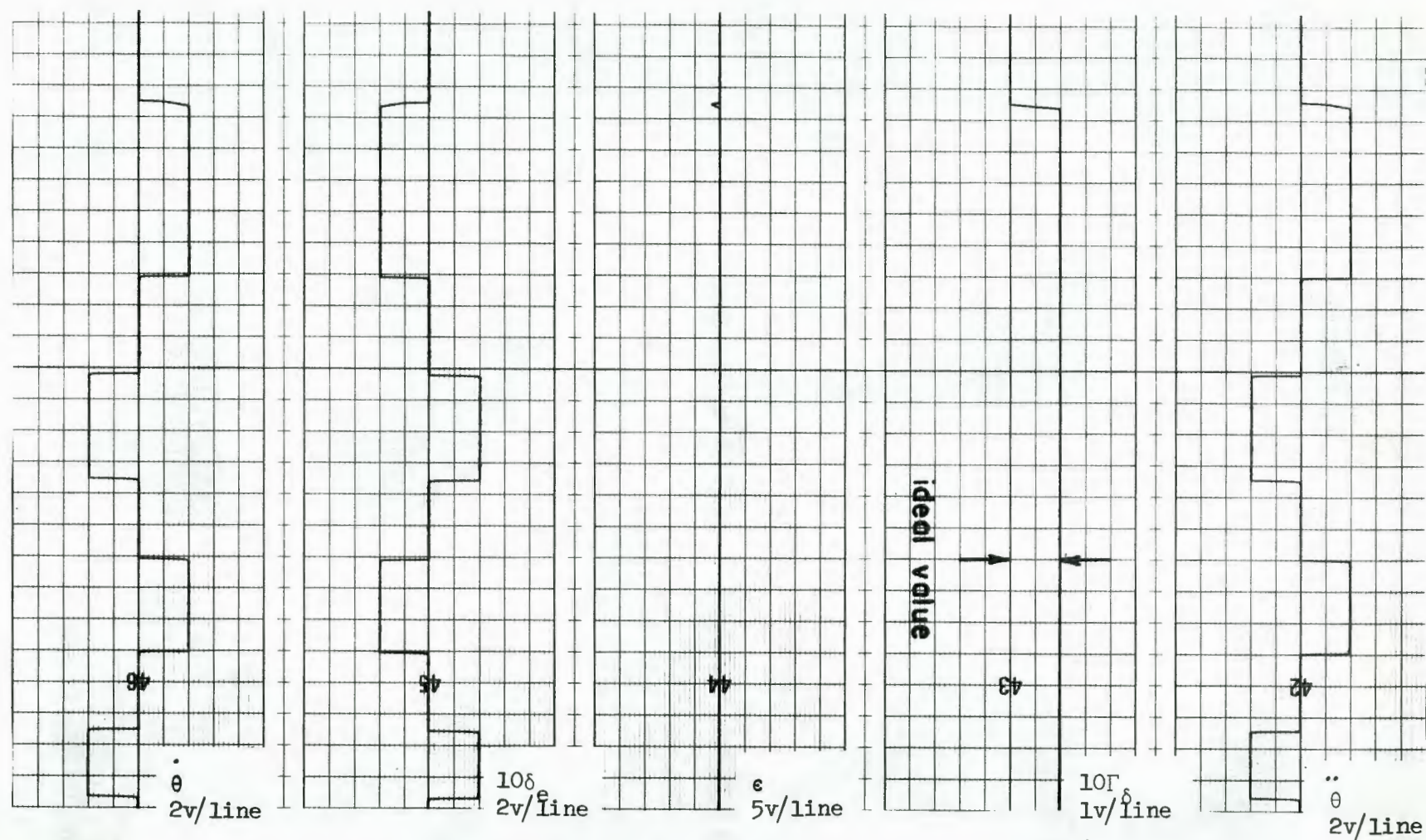


FIGURE 4. ANALOG TRACE FOR $\Gamma_\delta C$ -SYSTEM, WITHOUT SERVO $C_1=0$ $C_2=0$

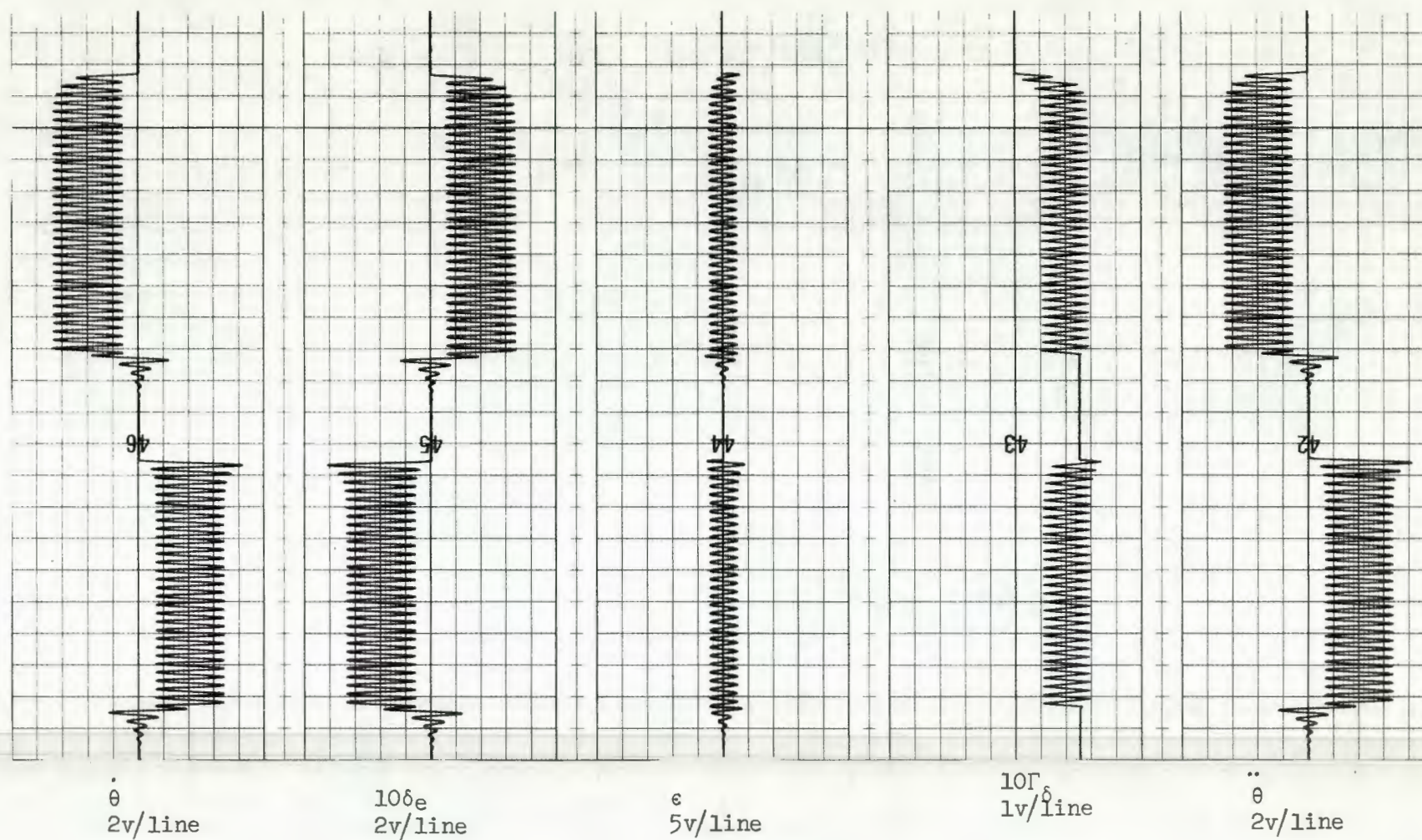


FIGURE 5. ANALOG TRACE FOR Γ_δ -SYSTEM, NEUTRAL STABILITY OSCILLATIONS
 $C_1=.47$ $C_2=.0039$

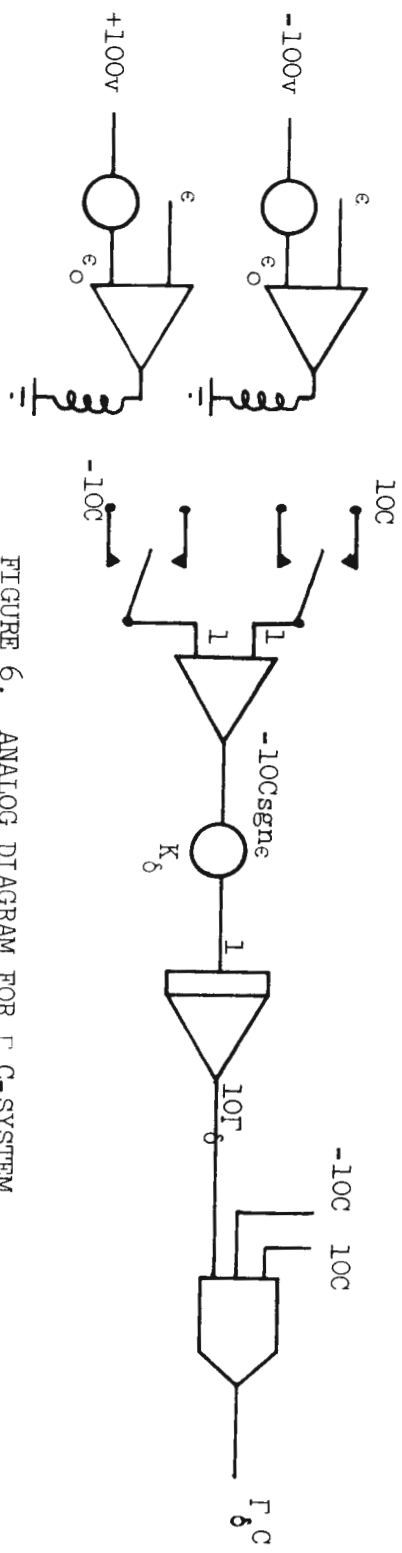
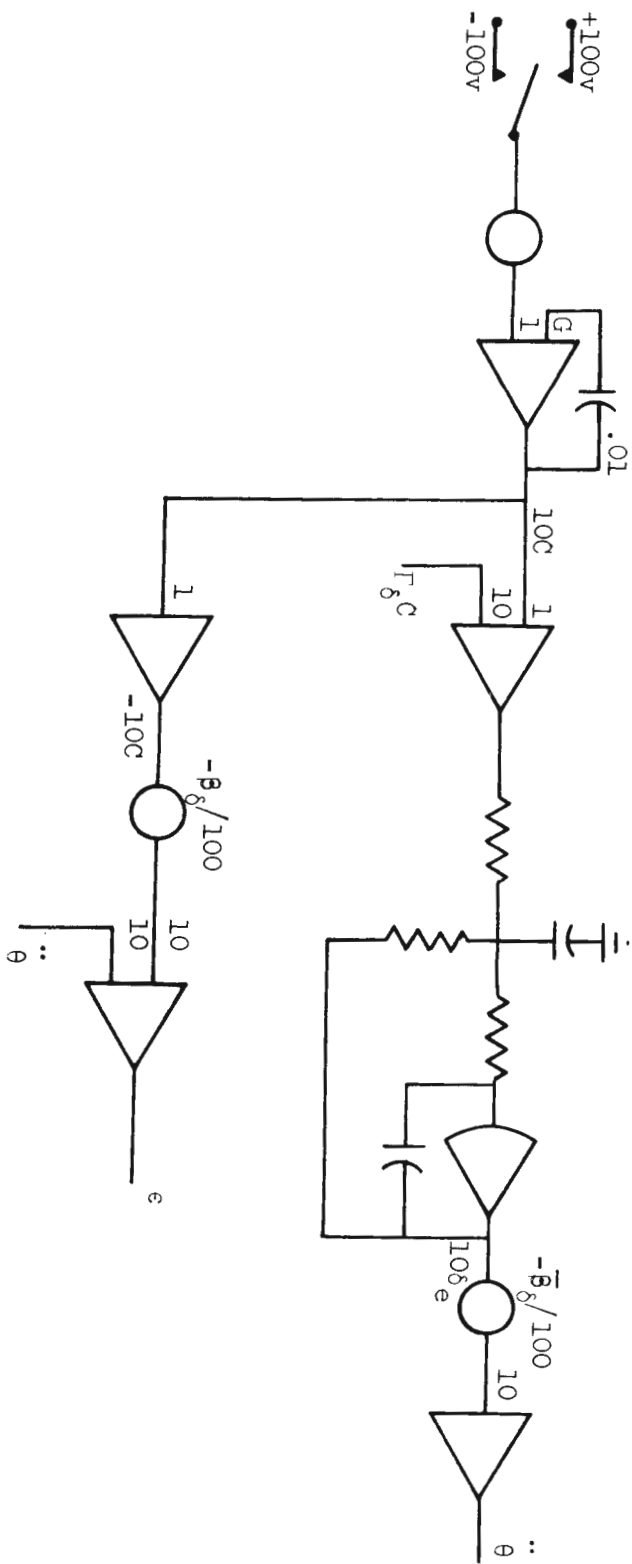


FIGURE 6. ANALOG DIAGRAM FOR γ_{δ} -SYSTEM

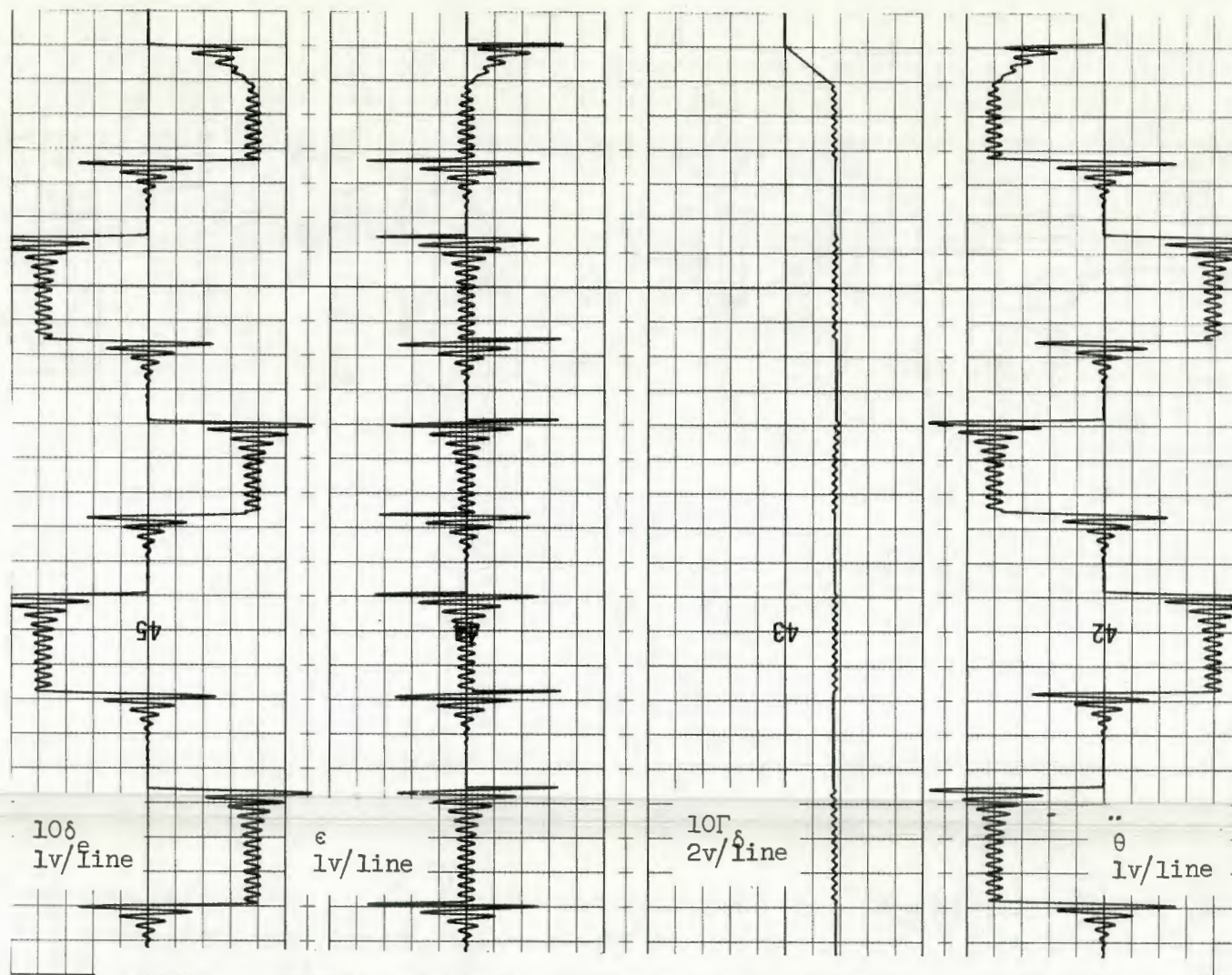


FIGURE 7. ANALOG TRACE FOR Γ_δ C-SYSTEM, LIMIT CYCLE OSCILLATIONS (RELAY)
 $C_1 = .47$ $C_2 = .0039$

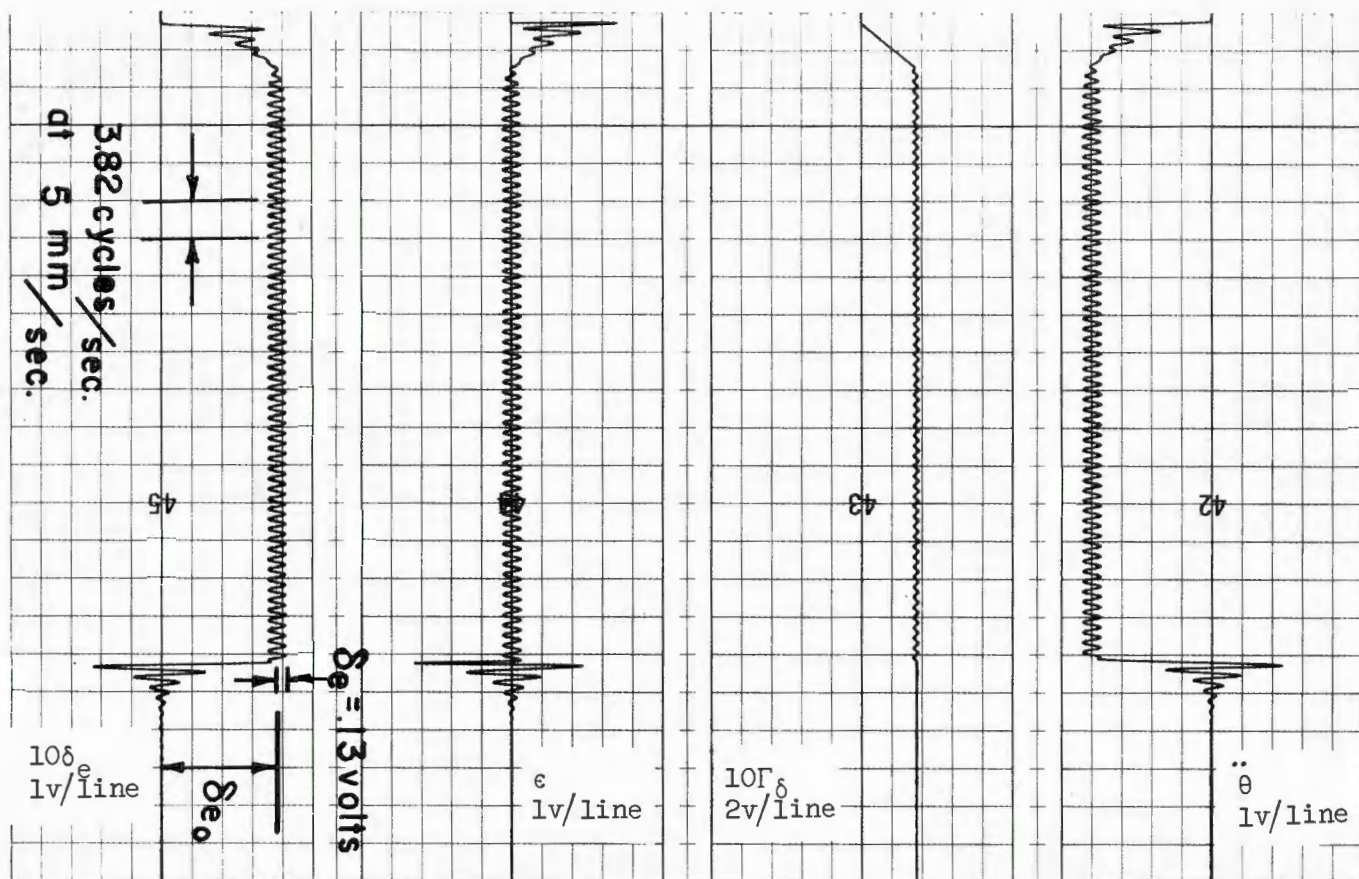


FIGURE 8. ANALOG TRACE FOR Γ_δ C-SYSTEM, LIMIT CYCLE OSCILLATIONS (RELAY)
 $C_1 = .47$ $C_2 = .0039$

$$\frac{d\Gamma_q}{dt} = K_q \dot{\theta} \epsilon \quad (G=\epsilon)$$

$$\ddot{\delta}_e + 2\zeta\omega\dot{\delta}_e + \omega^2\delta_e = \omega^2\bar{\delta}_e.$$

The block diagram is shown in Figure 9. Combining the equations gives:

$$\frac{d\Gamma_q}{dt} = K_q \dot{\theta} \left[(\bar{\beta}_q - \beta_\delta) \dot{\theta} + (\delta_e - C) \beta_\delta \right]$$

$$\ddot{\delta}_e + 2\zeta\omega\dot{\delta}_e + \omega^2\delta_e = \omega^2(C + \Gamma_q \dot{\theta})$$

$$\ddot{\theta} = \bar{\beta}_q \dot{\theta} + \beta_\delta \delta_e,$$

and applying the small perturbation theory

$$\Gamma_q = \Gamma_{q_0} + \hat{\Gamma}_q$$

$$\delta_e = \delta_{e_0} + \hat{\delta}_e$$

$$\dot{\theta} = \dot{\theta}_0 + \hat{\dot{\theta}}$$

yields the characteristic equation of the simplified $\Gamma_q \dot{\theta}$ system:

$$\lambda^4 - (\bar{\beta}_q - 2\zeta\omega)\lambda^3 - (2\zeta\omega\bar{\beta}_q - \omega^2)\lambda^2 - (\bar{\beta}_q\omega^2 + \beta_\delta\omega^2\Gamma_{q_0} + \beta_\delta K_q \dot{\theta}_0^2 \omega^2)\lambda + K_q \omega^2 \dot{\theta}_0^2 \beta_\delta \beta_q = 0,$$

$$\text{where } \Gamma_{q_0} = \frac{\beta_q - \bar{\beta}_q}{\beta_\delta} \quad \text{and} \quad \dot{\theta}_0 = \frac{-C_0 \beta_\delta}{\beta_q}.$$

Therefore the system is stable if

$$- (\beta_q \omega^2 + \frac{K_q \omega^2 C_0^2 \beta_\delta^3}{\beta_q^2}) (2\zeta\omega\bar{\beta}_q - \omega^2) (\bar{\beta}_q - 2\zeta\omega) > (\beta_q \omega^2 + \frac{K_q \omega^2 C_0^2 \beta_\delta^3}{\beta_q^2}) + (\bar{\beta}_q - 2\zeta\omega)^2 (\frac{K_q \omega^2 C_0^2 \beta_\delta^3}{\beta_q^2})$$

and limit cycles will not occur. It is obvious from the preceding stability relationship for the $\Gamma_q \dot{\theta}$ -controller that the equations for the complete control system are too complex to analyze. The $\Gamma_q \dot{\theta}$ -system is, however, sufficiently similar to the complete controller that most

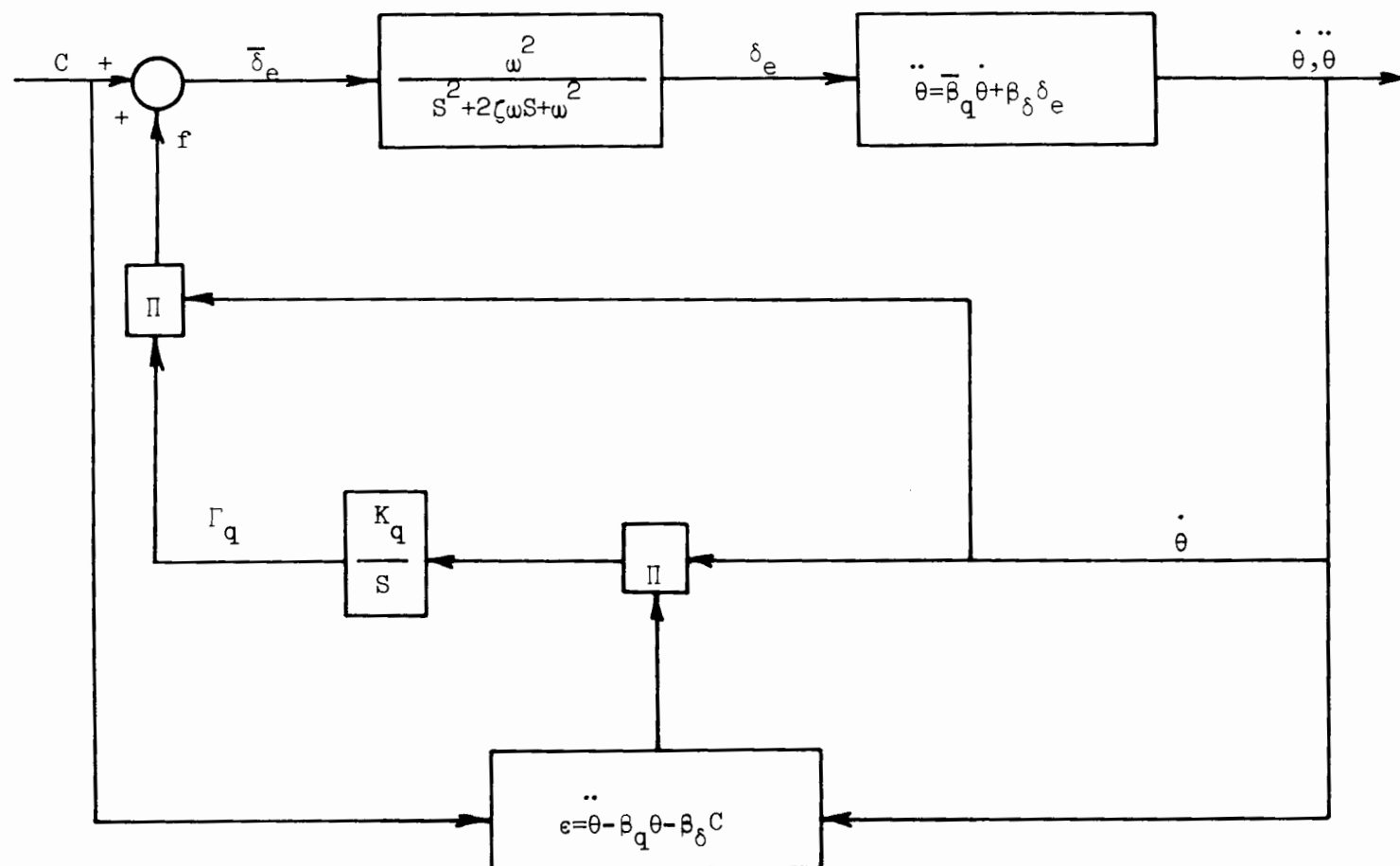


FIGURE 9. BLOCK DIAGRAM FOR SIMPLIFIED $\Gamma_q \dot{\theta}$ -CONTROL SYSTEM

of the analysis is applicable to both systems, as may be seen by analog simulation.

The $\Gamma_q \dot{\theta}$ -system was first operated without the servo and as the error approached zero, the variable gain approached its ideal value, Figure 10. The second order servo was again simulated by the circuit shown in Figure 3 and with $G = \epsilon$, the decade capacitor boxes were set to give the system neutral stability. The resulting motion is shown in Figure 11. With $G = \text{sgn}\epsilon$, a relay was used and the analog diagram for the system is shown in Figure 12. With sufficiently large inputs the system becomes unstable. This results in the limit-cycle oscillations shown in Figure 13.

The complete nonvarying- C^* adaptive control system was then patched on the analog computer according to the diagram shown in Figure 14. In Reference 1, Rang shows that the equations for the controller are somewhat more complicated than those derived in Chapter II resulting from the introduction of the actuator and actuator model. The complications resulting from the actuator and the second order servo will be shown in the following analog graphs. Figure 15 shows the free aircraft, that is the aircraft without the control function feedback loop, with no actuator. Figure 16 shows the free aircraft with the actuator. The effect of the actuator, considered as a first order lag $1/.1S+1$, may be seen by comparing $\ddot{\theta}$ and δ_e on the two preceding figures. Figures 17 and 18 show aircraft parameters of the complete adaptive control system without the actuator or actuator model and Figures 19 and 20 show the system parameters with the actuator and actuator model. As can be seen from these figures the variable gains do not approach the same value for the controller with and without the actuator. Thus the introduction of the

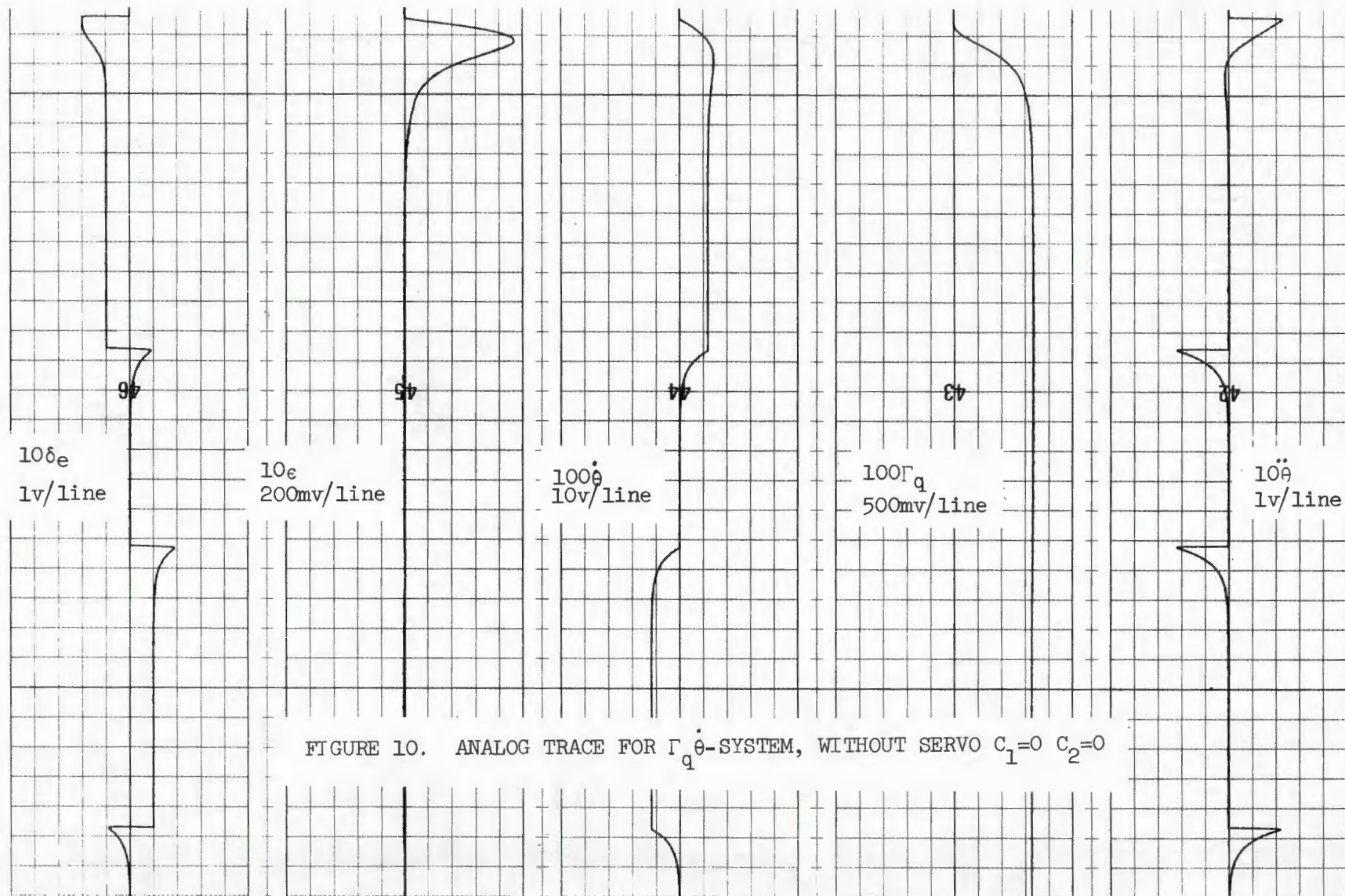


FIGURE 10. ANALOG TRACE FOR $\Gamma_q \dot{\theta}$ -SYSTEM, WITHOUT SERVO $C_1=0$ $C_2=0$

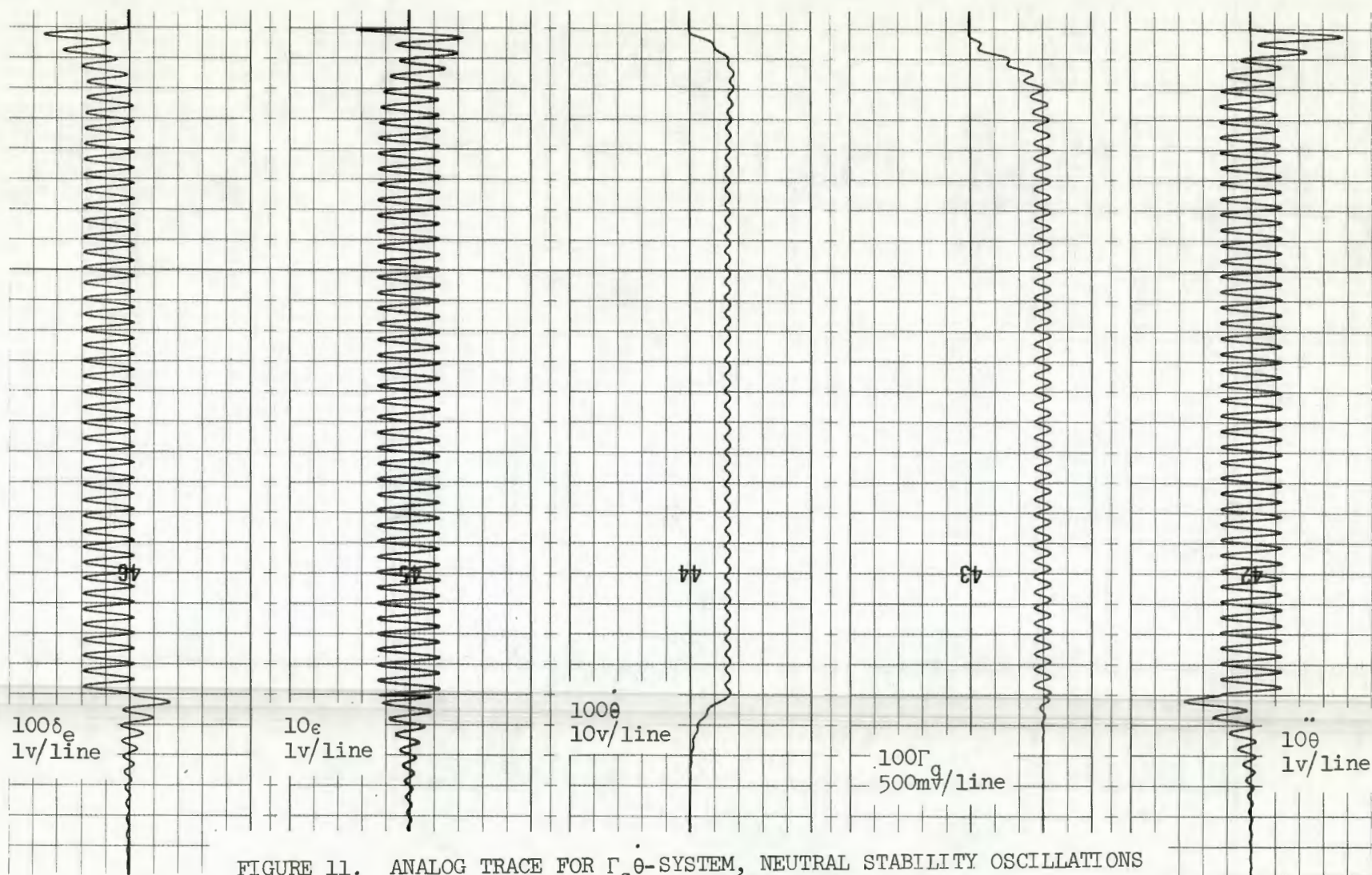


FIGURE 11. ANALOG TRACE FOR Γ_q -SYSTEM, NEUTRAL STABILITY OSCILLATIONS
 $C_1=1.28$ $C_2=.005$

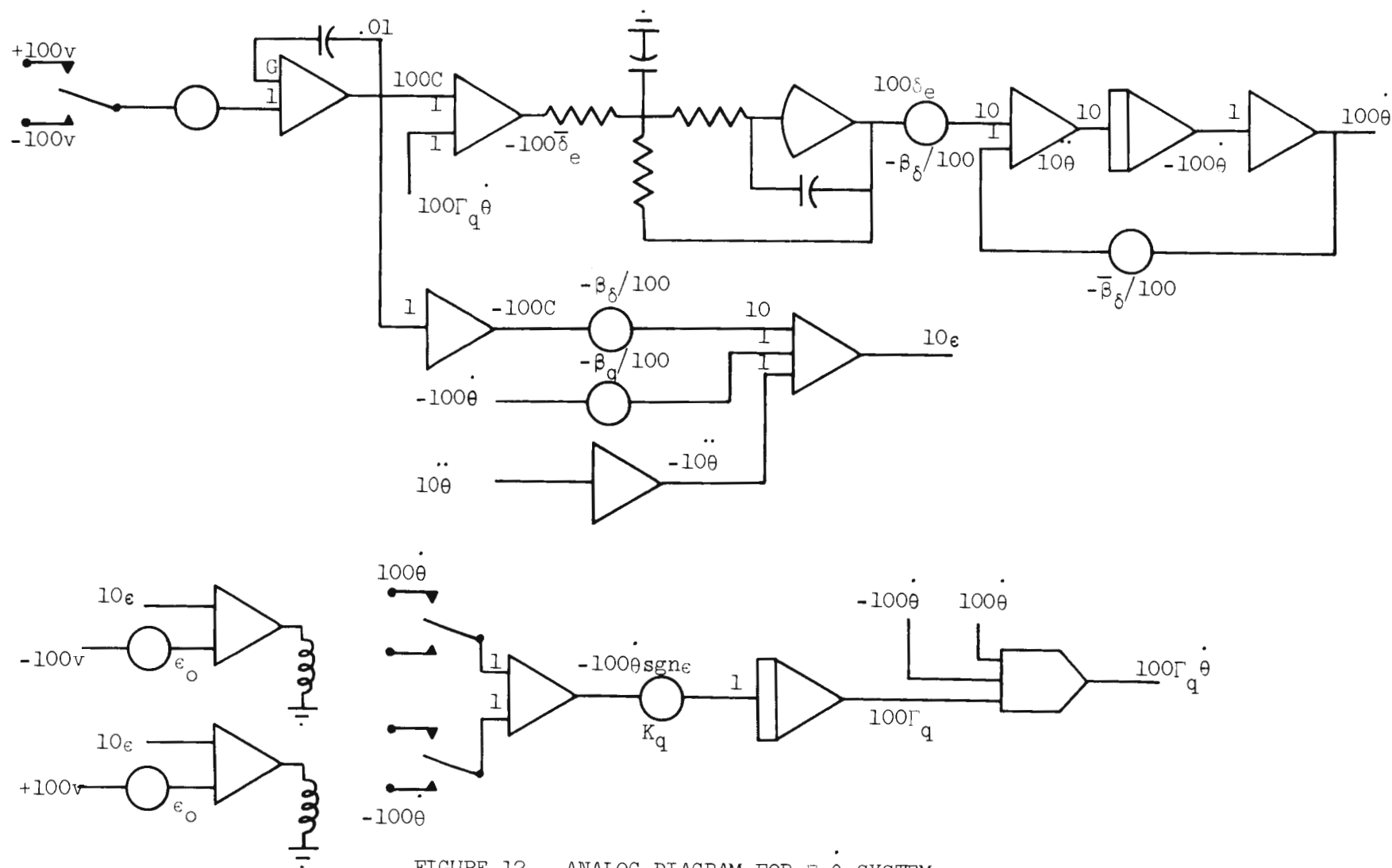


FIGURE 12. ANALOG DIAGRAM FOR $\Gamma_q \dot{\theta}$ -SYSTEM

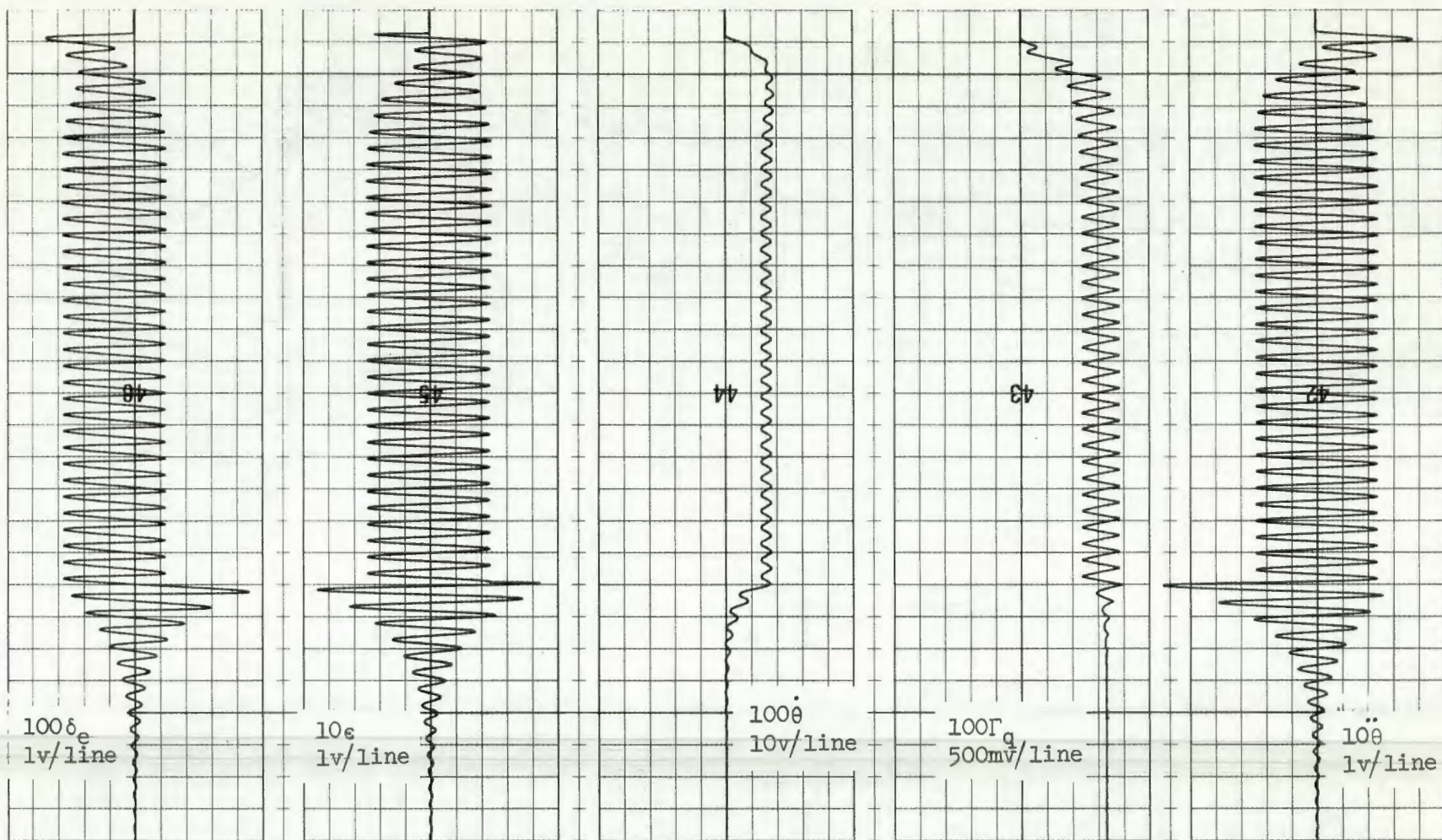


FIGURE 13. ANALOG TRACE FOR $\Gamma_q \dot{\theta}$ -SYSTEM, LIMIT CYCLE OSCILLATIONS (RELAY)
 $C_1=1.28$ $C_2=.005$

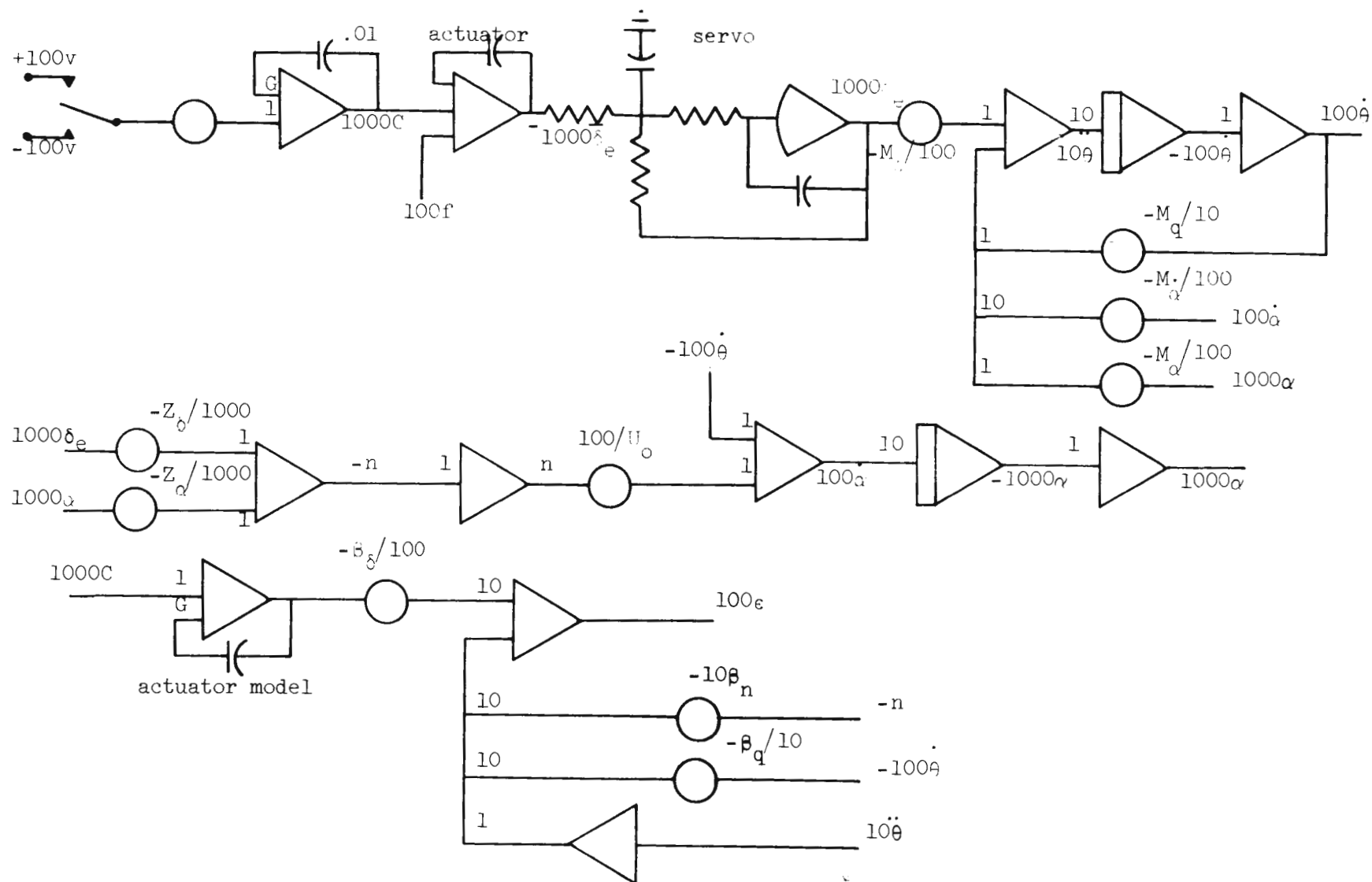


FIGURE 14. ANALOG DIAGRAM FOR NONVARYING-CONTROL SYSTEM

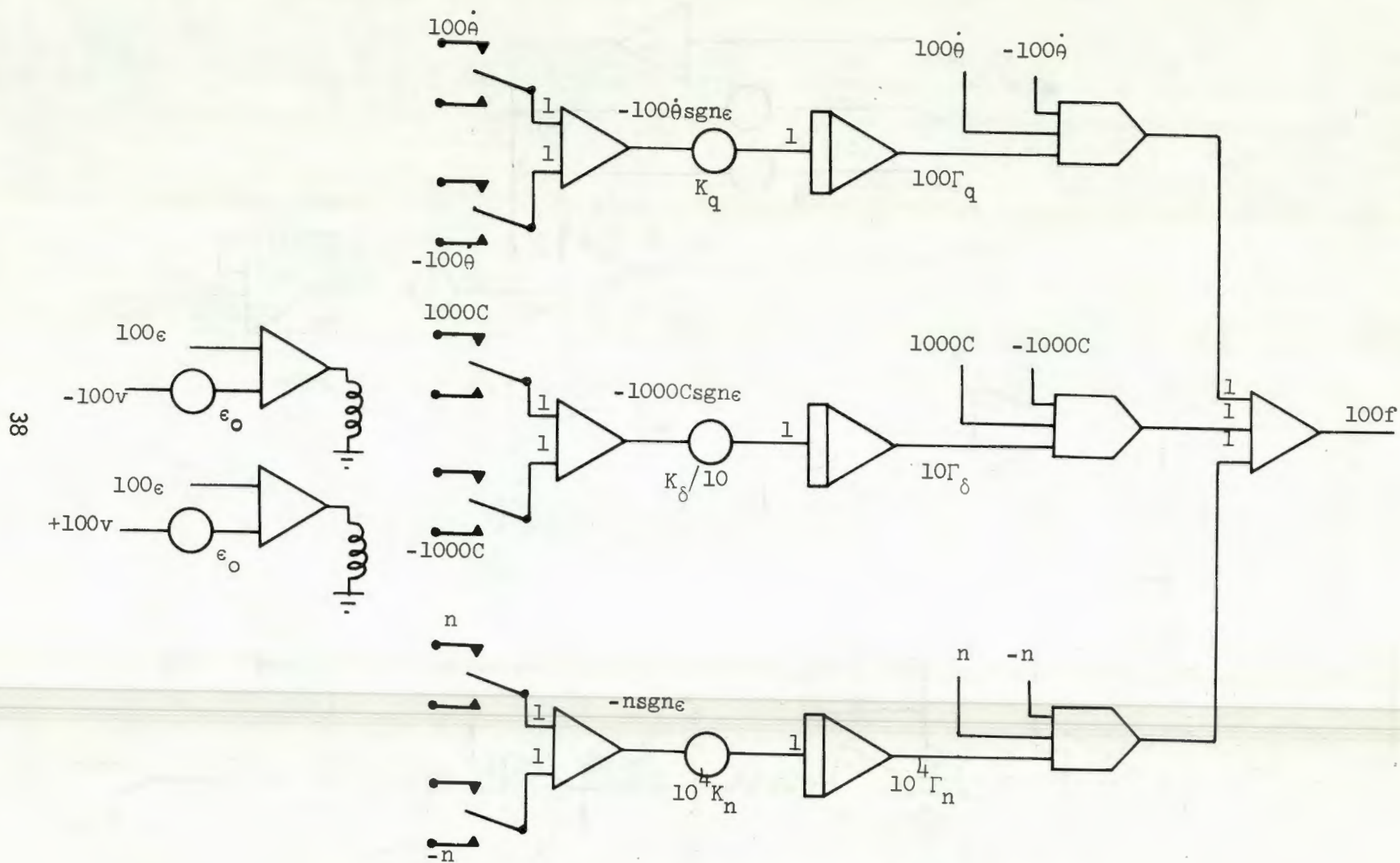


FIGURE 14. ANALOG DIAGRAM FOR NONVARYING- C^* CONTROL SYSTEM

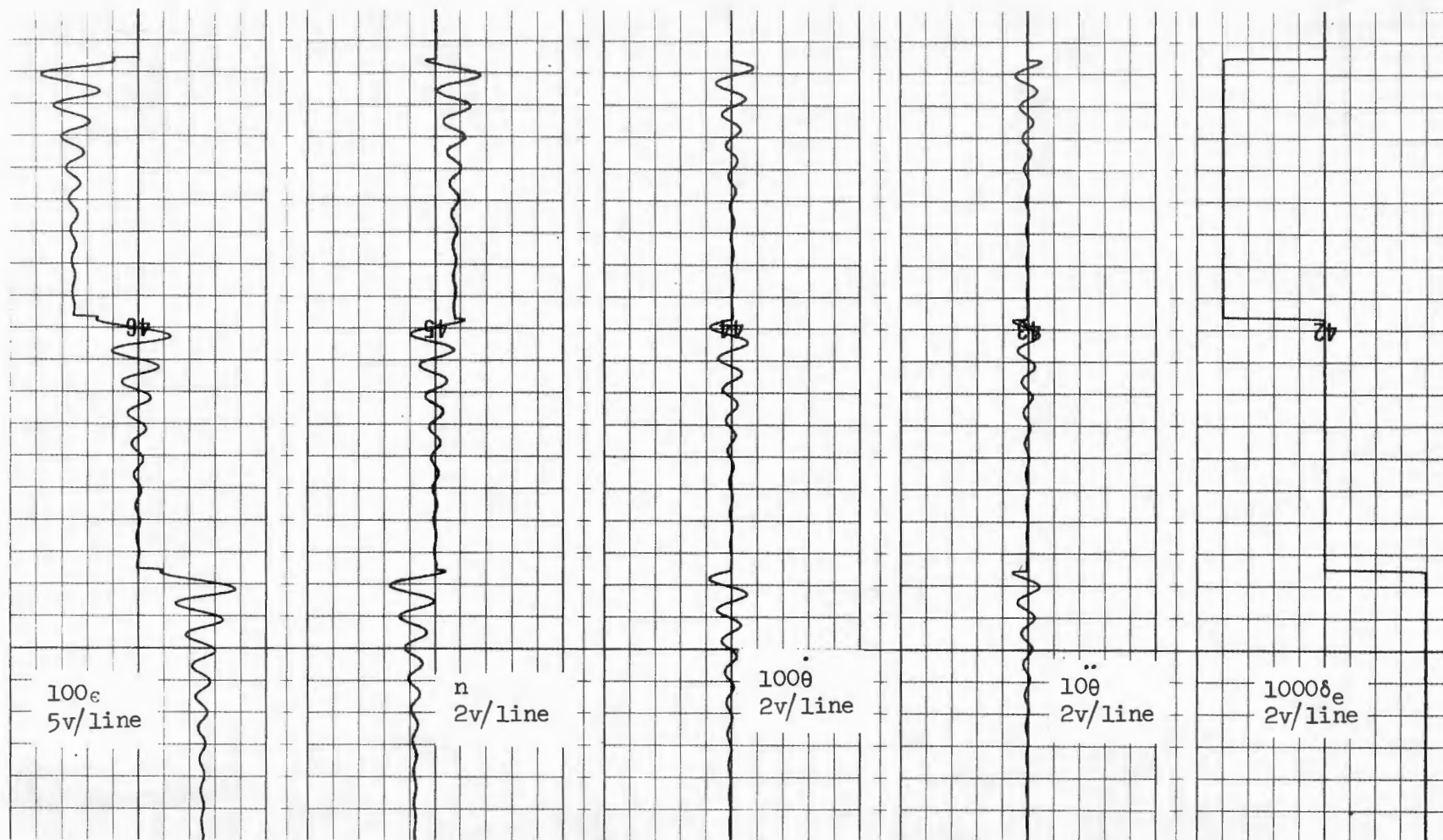
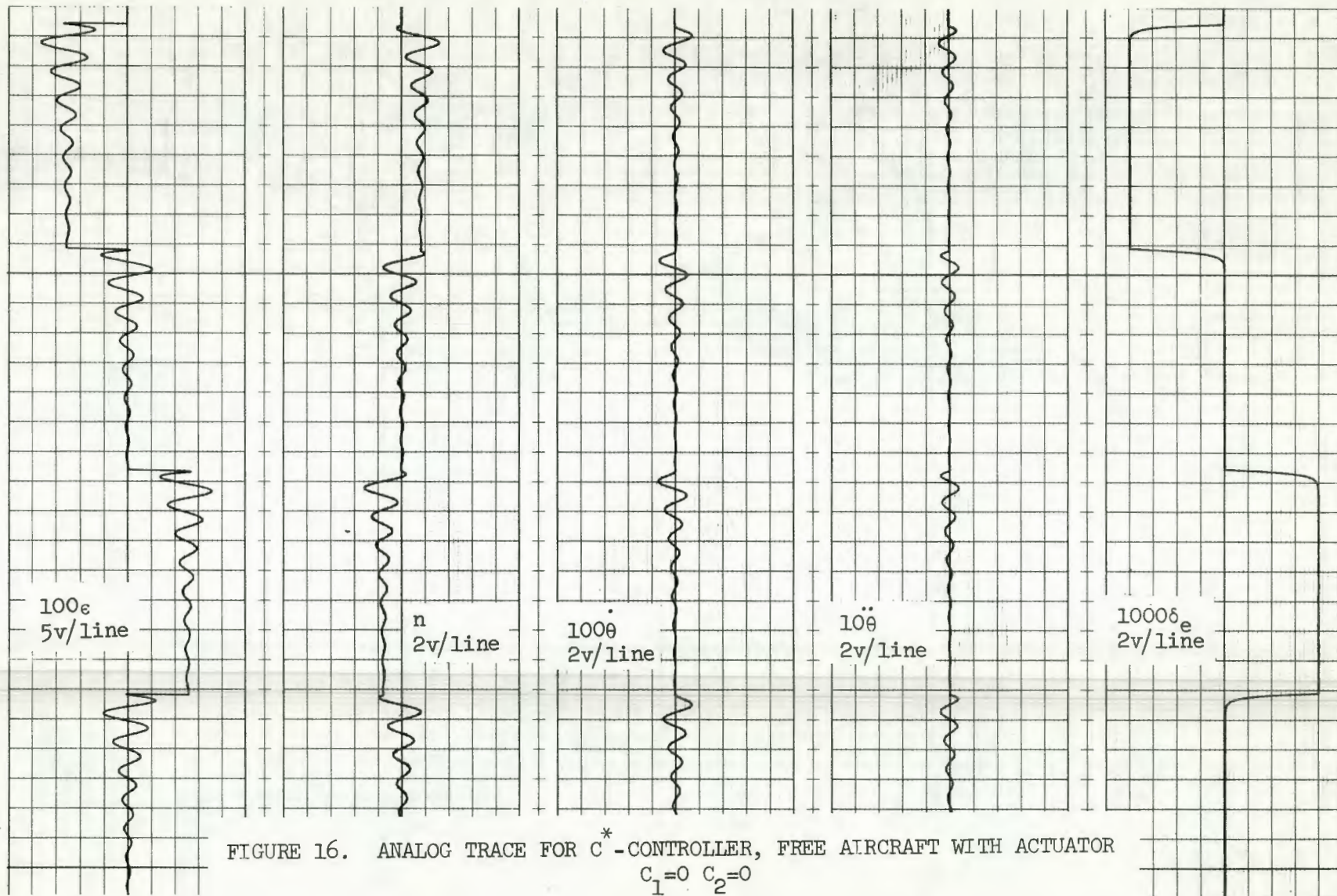


FIGURE 15. ANALOG TRACE FOR C^* -CONTROLLER, FREE AIRCRAFT WITHOUT ACTUATOR
 $C_1=0$ $C_2=0$



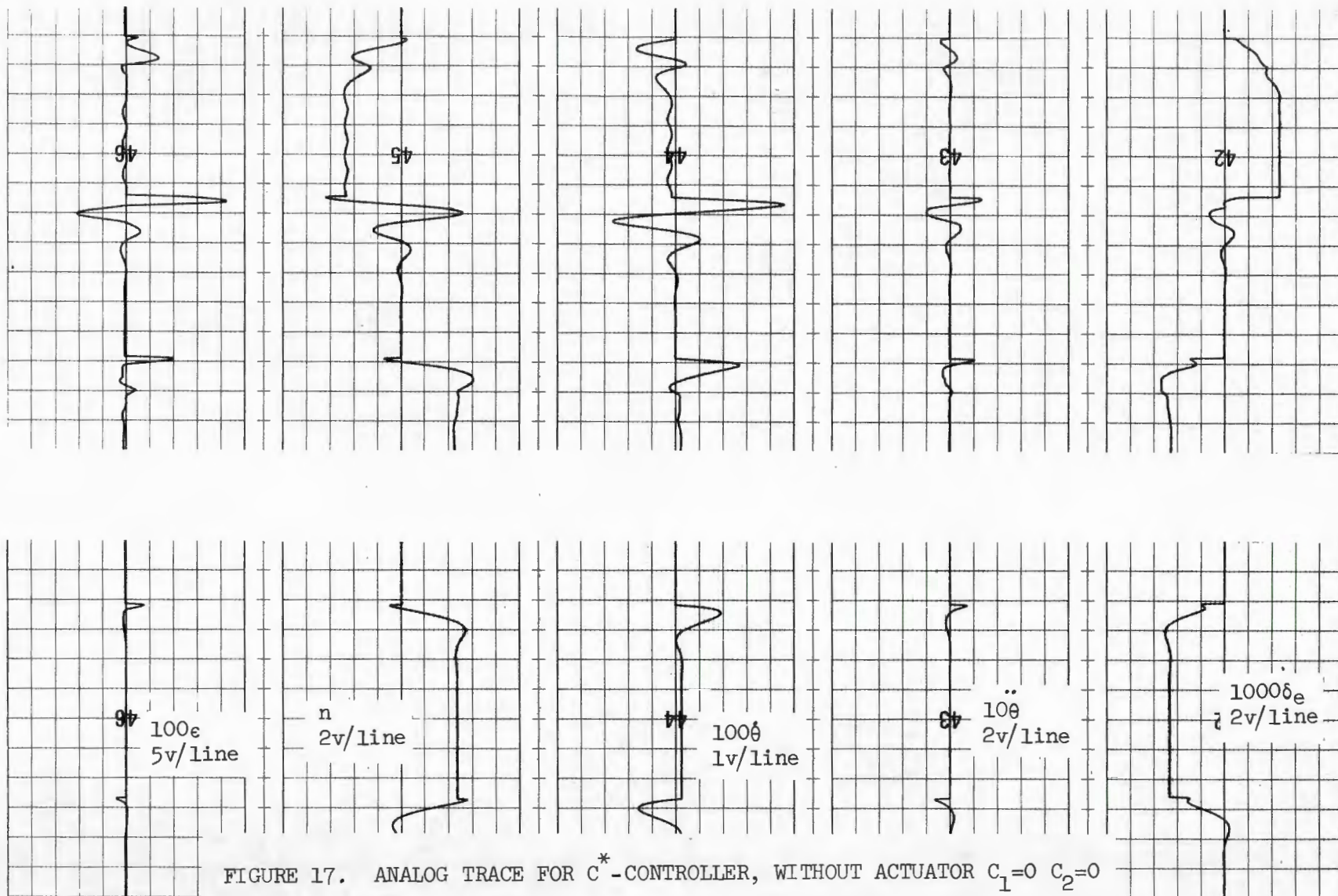
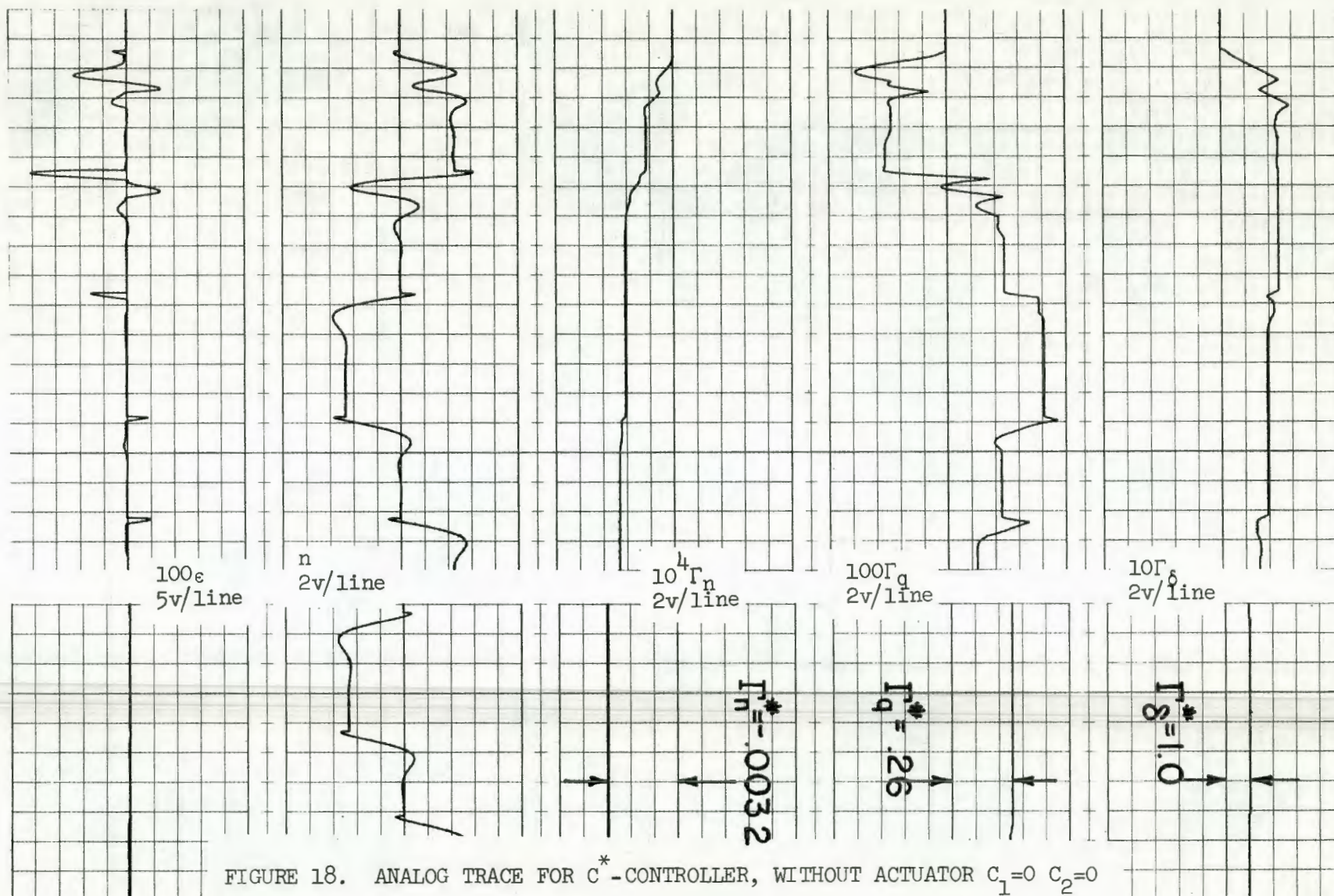


FIGURE 17. ANALOG TRACE FOR C^* -CONTROLLER, WITHOUT ACTUATOR $C_1=0$ $C_2=0$



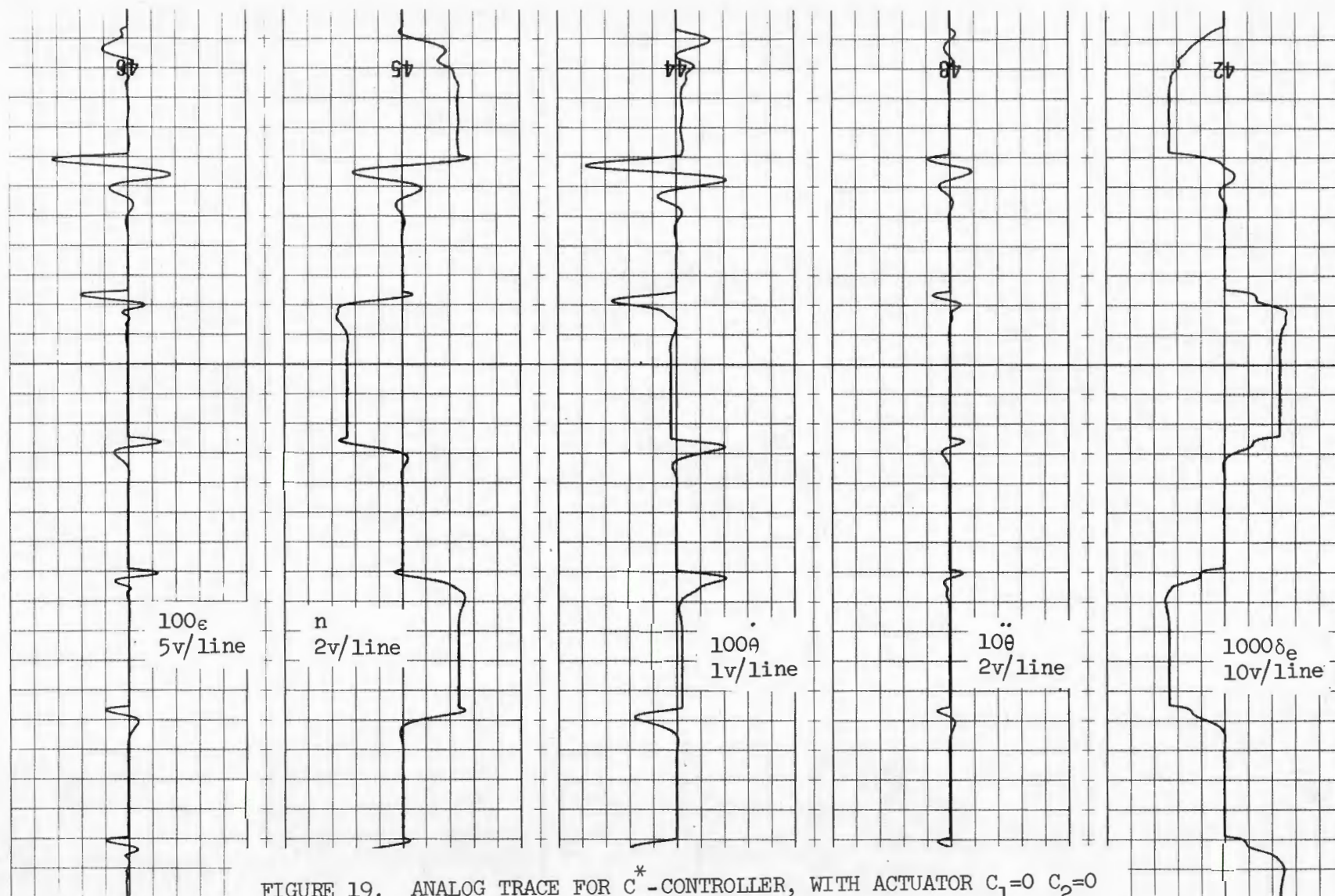


FIGURE 19. ANALOG TRACE FOR C^* -CONTROLLER, WITH ACTUATOR $C_1=0$ $C_2=0$

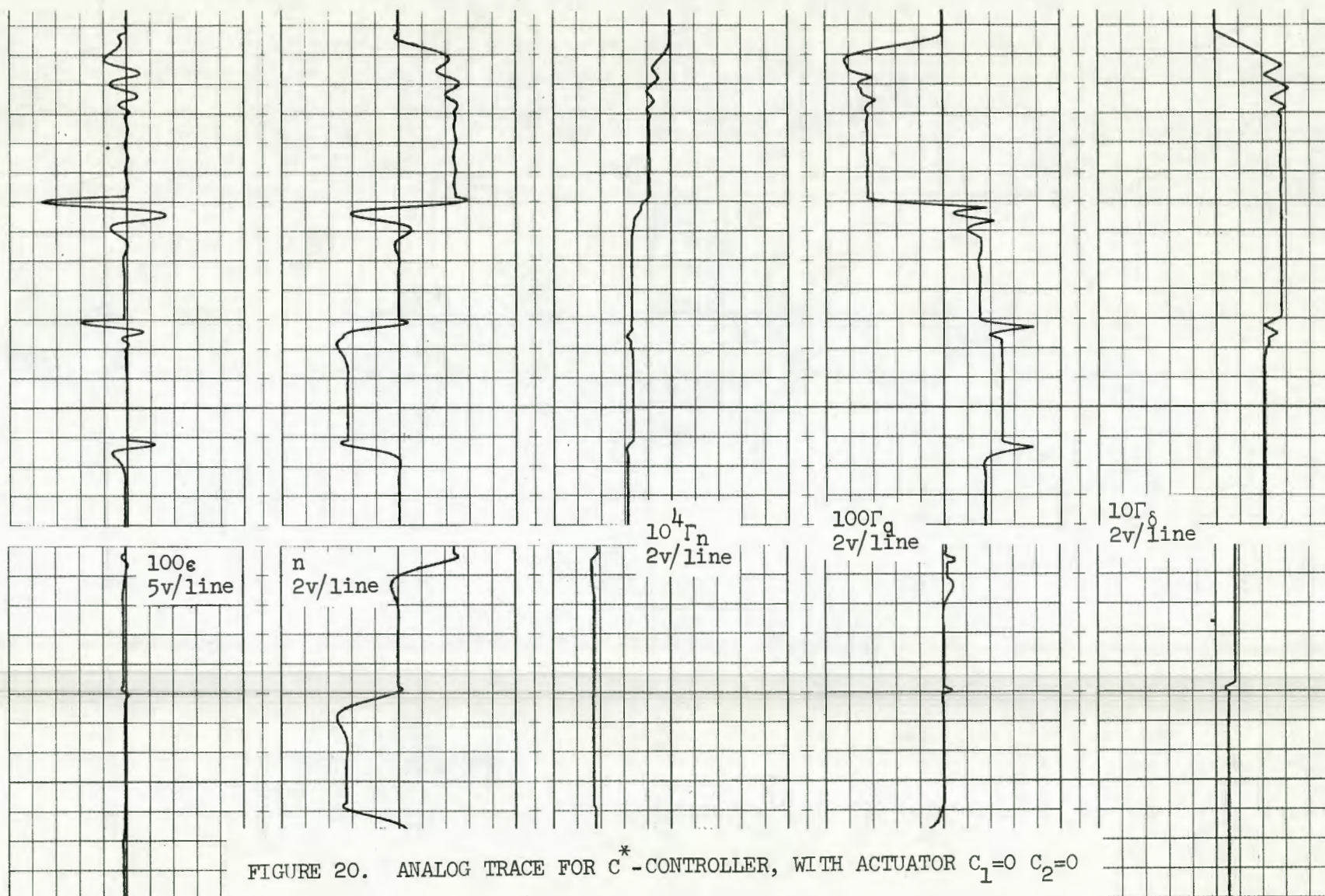


FIGURE 20. ANALOG TRACE FOR C^* -CONTROLLER, WITH ACTUATOR $C_1=0$ $C_2=0$

actuator has so complicated the control system that it no longer behaves as if its governing equation were exactly that of the criterion as the system error approaches zero. As soon as the second order servo is introduced into the system, the combined complications produce limit cycle oscillations as shown in Figure 21. It can thus be seen that the servo and actuator lags are complicating the system and causing the limit cycles.

The results obtained for the complete nonvarying-C* adaptive controller without the actuator or servo may be verified by calculating values of the variable gains based on the aircraft parameters for the F-4 aircraft. Figure 18 shows the complete adaptive controller without the complications introduced by the actuator or the servo at a flight condition of Mach 2.0 at 50,000 feet. Flight Condition 3 on Table I contains aircraft parameters for the F-4 aircraft at this same flight condition. Therefore, using the values of the ideal variable gains calculated from these aircraft parameters and listed on Table II, a comparison may be made to the values obtained by analog simulation, Figure 18. The values correspond closely which indicates that at this flight condition the variable gains are approaching their ideal values and the error is approaching zero. Similar results were obtained for all flight conditions which indicates that the basic controller is operating properly and limit cycles will not appear. Only with the actuator and series servo in the system, which is the case in the actual aircraft control system, will limit cycles appear.

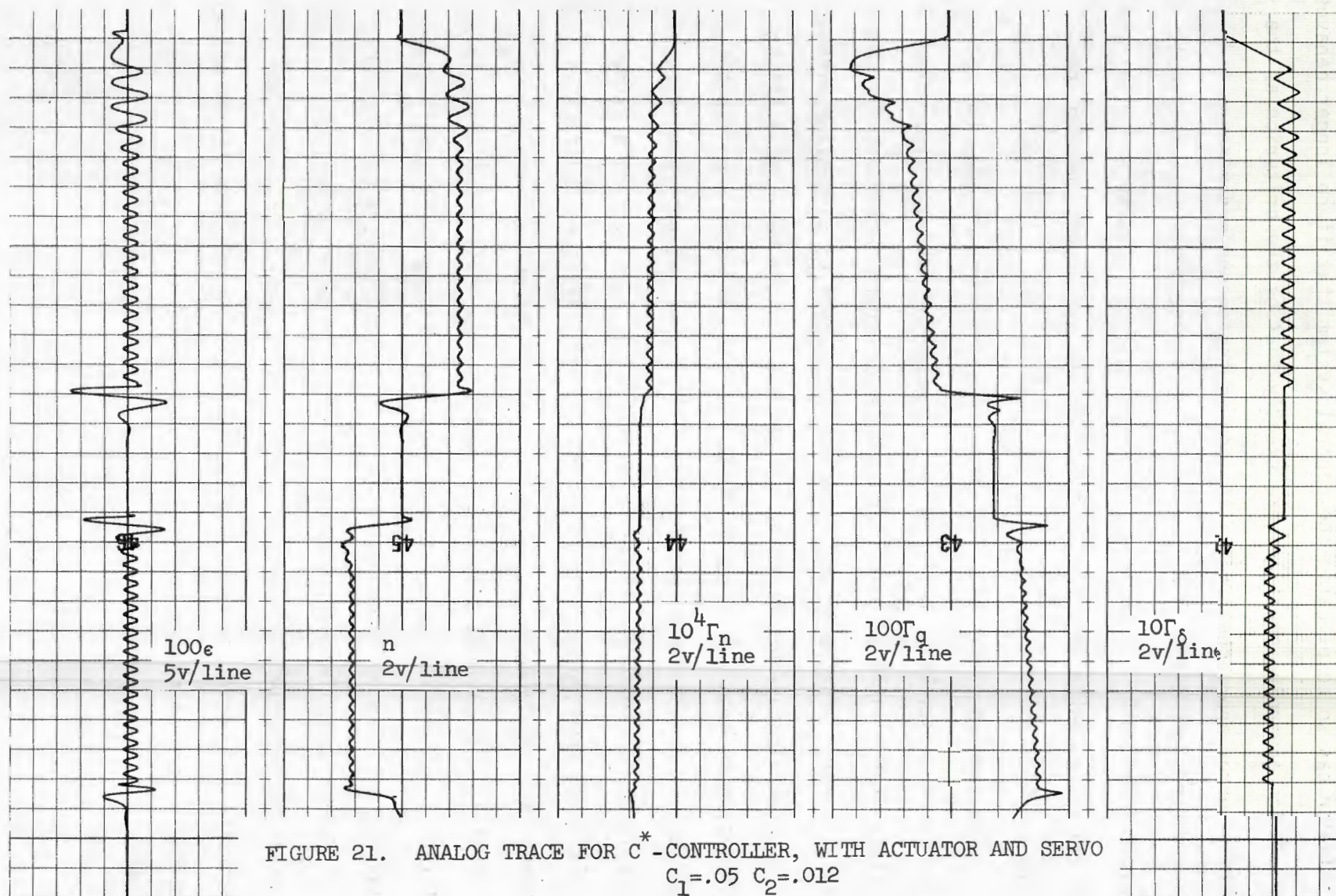


FIGURE 21. ANALOG TRACE FOR C^* -CONTROLLER, WITH ACTUATOR AND SERVO
 $C_1=.05$ $C_2=.012$

TABLE I
AIRCRAFT AND CONTROLLER PARAMETERS, F-4 AIRCRAFT
(units in radians, feet, seconds)

Flight Condition	1	2	3
Altitude	Sea Level	Sea Level	50,000
Mach No.	0.200	0.900	2.000
$100/U_0$	0.451	0.100	0.052
$-M_{\alpha}/100$	0.013	0.380	0.424
$-M_{\dot{\alpha}}/10$	0.026	0.139	0.004
$-M_q/10$	0.043	0.261	0.048
$-M_{\delta}/100$	0.028	0.584	0.149
$-Z_{\alpha}/1000$	0.083	2.420	0.817
$-Z_{\delta}/1000$	0.0131	0.314	0.102
$-\beta_{\delta}/100$	0.200	0.200	0.200
$-\beta_q/10$	0.300	0.300	0.300
$-10\beta_n$	0.200	0.200	0.200
$K_{\delta}/100$	0.999	0.999	0.999
$10^4 K_n$	0.500	0.500	0.500
$K_q/10$	0.999	0.999	0.999
$-\bar{\beta}_n$	0.0146	0.0143	0.0519
$-\bar{\beta}_q$	0.690	4.000	0.520
$-\bar{\beta}_{\delta}$	2.580	53.500	9.610
ϵ_0	0.020	0.020	0.020

TABLE II
IDEAL VALUE OF VARIABLE GAINS

Flight Condition	1	2	3
Altitude	Sea Level	Sea Level	50,000
Mach No.	0.200	0.900	2.000
Original Nonvarying-C* Controller			
Γ_{δ}^*	6.750	-0.630	1.080
Γ_q^*	0.900	-0.019	0.260
Γ_n^*	0.0021	0.0001	-0.0033
Modified Nonvarying-C* Controller			
Γ_{δ}^*	7.750	0.370	2.180
Γ_q^*	0.1155	-0.050	0.124
Γ_n^*	0.00027	0.00029	-0.00159

IV. STUDY OF LIMIT CYCLES AND POSSIBLE FIXES

In order to find fixes for the problem of limit cycle oscillations in a control system, the limit cycles must first be studied to find their amplitude and frequency. The combined equations for the controller using $G = \text{sgn} \epsilon$ are

$$\frac{d\Gamma_{\delta}}{dt} = K_{\delta} C \text{sgn} [\bar{\beta}_{\delta} \delta_e - \beta_{\delta} C]$$

$$\ddot{\delta}_e + 2\zeta\omega\dot{\delta}_e + \omega^2\delta_e = \omega^2(C + \Gamma_{\delta}C)$$

for the simplified $\Gamma_{\delta}C$ -system. Since the amplitude and frequency of the parasitic oscillations on the steady state are desired, apply the small disturbance theory by setting

$$\Gamma_{\delta} = \Gamma_{\delta_0} + \hat{\Gamma}_{\delta}$$

$$\text{and } \delta_e = \delta_{e_0} + \hat{\delta}_e.$$

Setting $C = C_0$ and substituting in these perturbation equations gives the system's full variational equations

$$\frac{d\hat{\Gamma}_{\delta}}{dt} = K_{\delta} C_0 \text{sgn} [\bar{\beta}_{\delta} \hat{\delta}_e]$$

$$\frac{d^2\hat{\delta}_e}{dt^2} + 2\zeta\omega \frac{d\hat{\delta}_e}{dt} + \omega^2\hat{\delta}_e = \omega^2\hat{\Gamma}_{\delta}C_0$$

which may be combined to yield

$$\frac{d^3\hat{\delta}_e}{dt^3} + 2\zeta\omega \frac{d^2\hat{\delta}_e}{dt^2} + \omega^2 \frac{d\hat{\delta}_e}{dt} - \omega^2 C_0^2 K_{\delta} \text{sgn} [\bar{\beta}_{\delta} \hat{\delta}_e] = 0.$$

The method of Harmonic Balance, Reference 3, allows higher order harmonics to be disregarded if it is assumed that $\hat{\delta}_e = A \sin \Omega t$ + higher order harmonics. Making the proper substitutions for derivatives of $\hat{\delta}_e$ in the preceding equation yields

$$A\Omega(\Omega^2 - \omega^2)\cos\Omega t + 2\zeta\omega A\Omega^2\sin\Omega t + \omega^2 C_0^2 K_\delta \text{sgn}[\bar{\beta}_\delta A\sin\Omega t] = 0.$$

If the Describing Function for a relay with a deadband of $2\epsilon_0$ could be calculated, then it would be possible to eliminate the nonlinear term $\text{sgn}[A\sin\Omega t]$. According to Gibson, Reference 4, the Describing Function for such a relay is $k\sin(\Omega t + \Phi)$, where $K = \frac{4}{\pi A} \cos(\sin^{-1} \frac{\epsilon_0}{A\bar{\beta}_\delta})$ and $\Phi = 0$ for this system. Making this substitution gives

$$A\Omega(\Omega^2 - \omega^2)\cos\Omega t + (2\zeta\omega A\Omega^2 - \omega^2 C_0^2 K_\delta \frac{4}{\pi} \cos(\sin^{-1} \frac{\epsilon_0}{A\bar{\beta}_\delta})) \sin\Omega t = 0.$$

Setting the coefficients of $\cos\Omega t$ and $\sin\Omega t$ equal to zero yields equations for frequency and amplitude of the limit cycle oscillations, $\Omega = \omega$

$$A = \left\{ \frac{K}{2} [\bar{K} \pm (\bar{K}^2 - 4\epsilon_0^2/\bar{\beta}_\delta^2)^{1/2}] \right\}^{1/2}$$

where $\bar{K} = 2C_0^2 K_\delta / \zeta\omega\pi$. Figure 8 shows limit cycle oscillations for the $\Gamma_\delta C$ -system with $C_1 = .47$ and $C_2 = .0039$ which corresponds to $\omega = 24$ rad/sec. and $\zeta = .14$. With $C_0 = 1$, $K_\delta = .7$, $\epsilon_0 = .2$, and $\bar{\beta}_\delta = -10$ values of Ω and A may be calculated from the preceding equations to be 3.82 cycles/second and .1311 volts respectively. Figure 8 confirms these values on the trace for $10\delta_e$. Since the frequency of the limit cycle oscillations is now known, it is known what frequencies may be filtered or where to apply a lead or lag compensation to possibly eliminate the limit cycles.

An investigation of why the oscillations are present in the first place, results in a better understanding of the problem at hand. From the set of equations for the $\Gamma_\delta C$ -system in Chapter II, it was observed that the ideal values for $\ddot{\theta}$ and Γ_δ were $\ddot{\theta} = \beta_\delta C$ and $\Gamma_\delta^* = \frac{\beta_\delta}{\bar{\beta}_\delta} - 1$. If a perturbed system is considered where $\ddot{\theta}$ and Γ_δ are at some small

disturbance quantity from their ideal values, the equations are

$$C = C_0$$

$$\Gamma_\delta = \frac{\beta_\delta}{\bar{\beta}_\delta} - 1 + \gamma$$

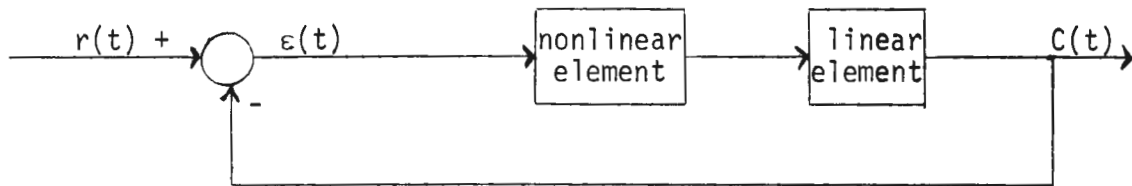
$$\varepsilon = \ddot{\theta} - \beta_\delta C_0$$

and the small disturbance terms ε and γ are driving the system until $\varepsilon = 0$, $\gamma = 0$; therefore $\ddot{\theta} = \beta_\delta C_0$ and $\Gamma_\delta = \Gamma_\delta^*$. Hence, from the system equations,

$$\beta_\delta C_0 + \varepsilon = \bar{\beta}_\delta \left[C_0 + \left(\frac{\beta_\delta}{\bar{\beta}_\delta} - 1 + \gamma \right) C_0 \right] \text{ and thus } \varepsilon = \bar{\beta}_\delta C_0 \gamma. \text{ The}$$

block diagram for the perturbed $\Gamma_\delta C$ -system is contained on Figure 22.

This figure shows that there will be a maximum phase shift of -270 degrees. It can also be shown that limit cycle oscillations occur at -180 degrees phase shift by the following simple diagram.



Assume,

$$\varepsilon(t) = A \sin \omega t$$

$$C(t) = A k \sin(\omega t + \Phi)$$

where k and Φ are the amplitude and phase angle of the combined non-linear and linear elements. In order for a periodic oscillation to occur, it can be seen that $\varepsilon(t)$ must equal $-C(t)$. Therefore, $-A \sin \omega t = A k \sin(\omega t + \Phi)$ and thus $k = 1$ and $\Phi = -180$ degrees, or the amplitude ratio must equal one and the phase shift must equal -180 degrees for limit cycle oscillations to appear. It was found that the frequency of the oscillations is $\Omega = \omega$; therefore, the Bode Plot for the simplified system would be as shown in Figure 23.

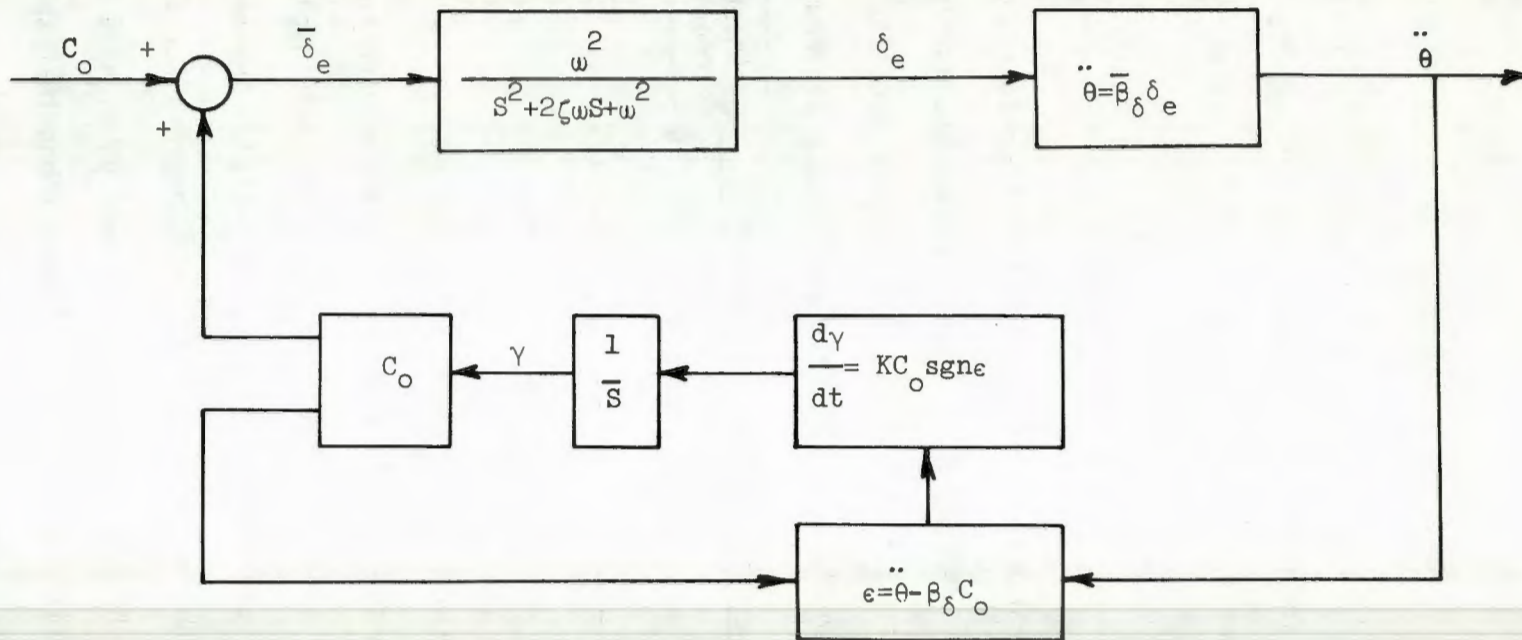
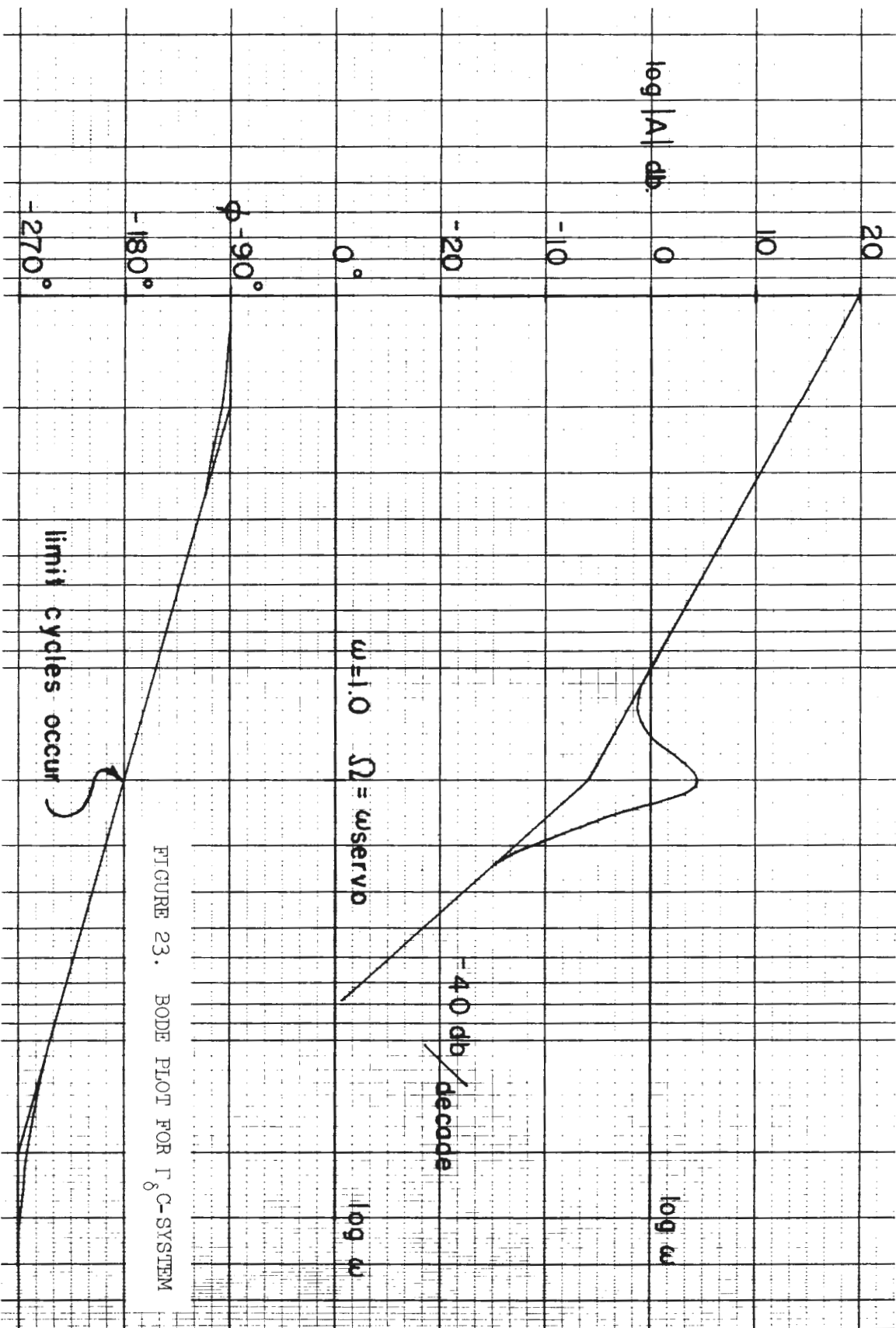


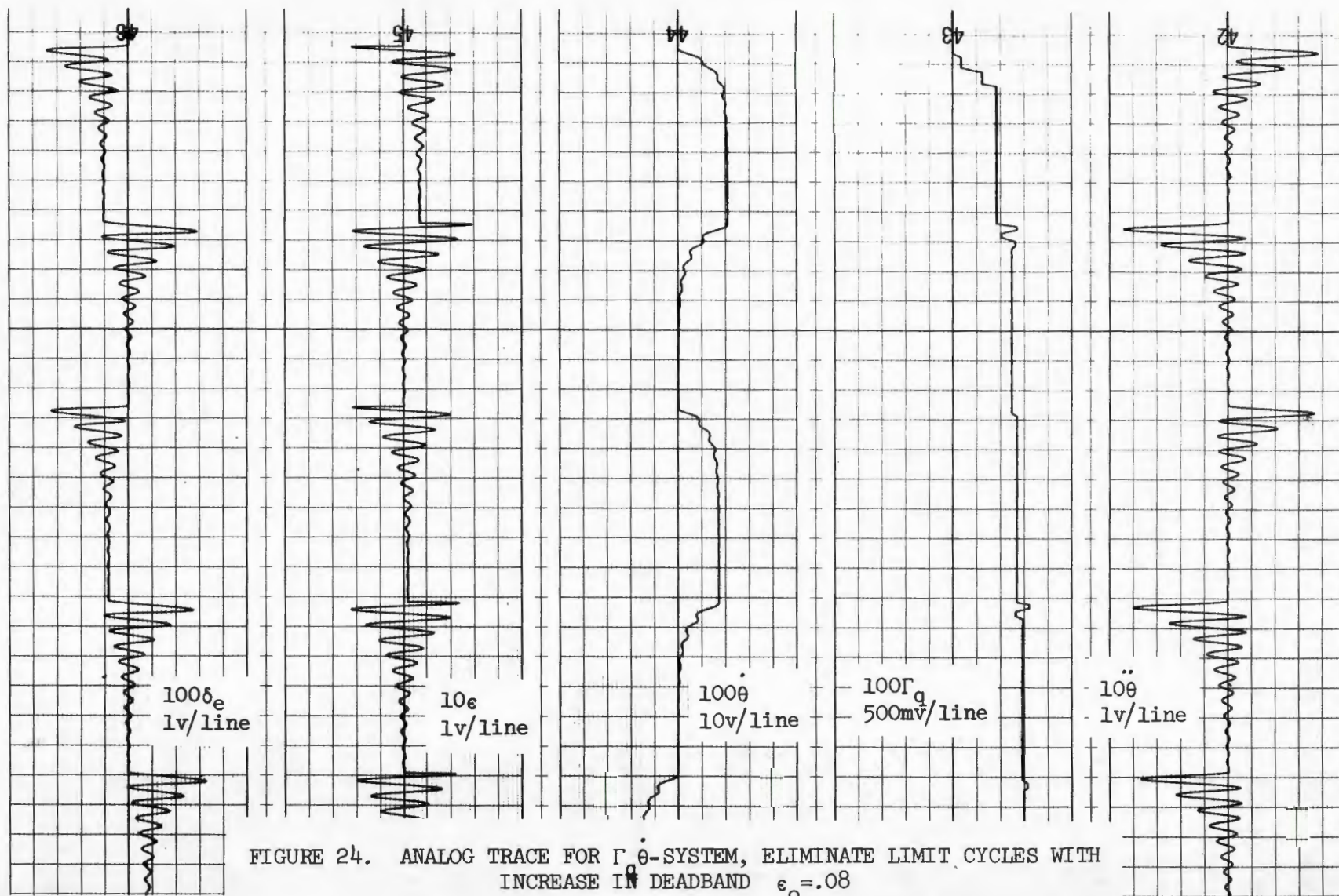
FIGURE 22. BLOCK DIAGRAM FOR PERTURBED $\Gamma_\delta C$ -SYSTEM.



It would appear from Figure 23 that lead, lag, or lead-lag compensations are not the answer to the problem since the phase shift will always go from -90 degrees to -270 degrees passing through -180 degrees. This was verified by analog simulation using different compensations. The amplitude and frequency of the limit cycles could be greatly altered but the oscillations, however small, still remained. Two fixes remained promising: 1) increase the deadband on the relay so that the oscillations present in the error signal would be within the relay deadband and would not drive the relay; and 2) alter the system so the phase shift never became greater than -180 degrees and thus limit cycles could not occur.

Figure 13 shows the inherent limit cycle oscillations characteristic of the $\Gamma_q \dot{\theta}$ -simplified-controller. When the relay deadband was increased from $\epsilon_0 = .02$ to $\epsilon_0 = .08$, the limit cycles completely disappeared. The system became stable and transients resulting from a step elevator deflection soon died out. Figure 24 shows the $\Gamma_q \dot{\theta}$ -system with $\epsilon_0 = .08$ and all other parameters remaining the same as in Figure 13; limit cycle oscillations are no longer present in the system. Although this fix works perfectly well, it is undesirable to make the oscillation free operation of the adaptive control system depend on the deadband size of the relay. If the deadband were made sufficiently large to eliminate limit cycles at the largest input command possible for safe aircraft operation, then the controller would be relatively nonresponsive at small input commands. This fine balance of deadband size would be most difficult to achieve and is therefore undesirable.

The second fix, altering the basic system to avoid making the phase shift pass through -180 degrees seemed a reasonable approach. If the



second order servo were taken out of the perturbed $\Gamma_\delta C$ -control loop shown in Figure 22, then the phase shift would go from 0 degrees to -90 degrees instead of from -90 degrees to -270 degrees and the phase shift would never pass through -180 degrees. Thus, the system would not exhibit limit cycle oscillations. This approach is considered in the next chapter.

V. MODIFICATION OF THE SIMPLIFIED $\Gamma_\delta C$ -CONTROLLER

If a second nonvarying- C^* control system could be developed similar to the first whose phase shift did not pass through -180 degrees, but whose variable gains approached their ideal values as the system error approached zero, then the new controller would be adaptive and would not exhibit limit cycles. Again, a simplified version of the complete system was studied first due to the complex nature of the system equations. The block diagram for the proposed altered $\Gamma_\delta C$ -system is shown in Figure 25. The set of equations which describe this system are

$$\ddot{\theta} = \bar{\beta}_\delta \delta_e$$

$$\varepsilon = \ddot{\theta} \Gamma_\delta - \beta_\delta \delta_e = [\bar{\beta}_\delta \Gamma_\delta - \beta_\delta] \delta_e$$

$$\frac{d\Gamma_\delta}{dt} = K_\delta \delta_e \operatorname{sgn} \varepsilon$$

$$\bar{\delta}_e = \Gamma_\delta C$$

$$\ddot{\delta}_e + 2\zeta\omega\dot{\delta}_e + \omega^2\delta_e = \omega^2\bar{\delta}_e.$$

Using the Gradient Technique, set

$$2v = \frac{1}{K_\delta} [\bar{\beta}_\delta \Gamma_\delta - \beta_\delta]^2$$

which comes from the error equation. Taking the derivative yields

$$\frac{dv}{dt} = \frac{1}{K_\delta} [\bar{\beta}_\delta \Gamma_\delta - \beta_\delta] \bar{\beta}_\delta \frac{d\Gamma_\delta}{dt}.$$

If $\frac{d\Gamma_\delta}{dt}$ is now chosen to be $\frac{d\Gamma_\delta}{dt} = K_\delta \delta_e \operatorname{sgn} \varepsilon$, then the gradient becomes

$$\frac{dv}{dt} = [\bar{\beta}_\delta \Gamma_\delta - \beta_\delta] \bar{\beta}_\delta \delta_e \operatorname{sgn} \varepsilon$$

$$\frac{dv}{dt} = \bar{\beta}_\delta \varepsilon \operatorname{sgn} \varepsilon = \bar{\beta}_\delta |\varepsilon|.$$

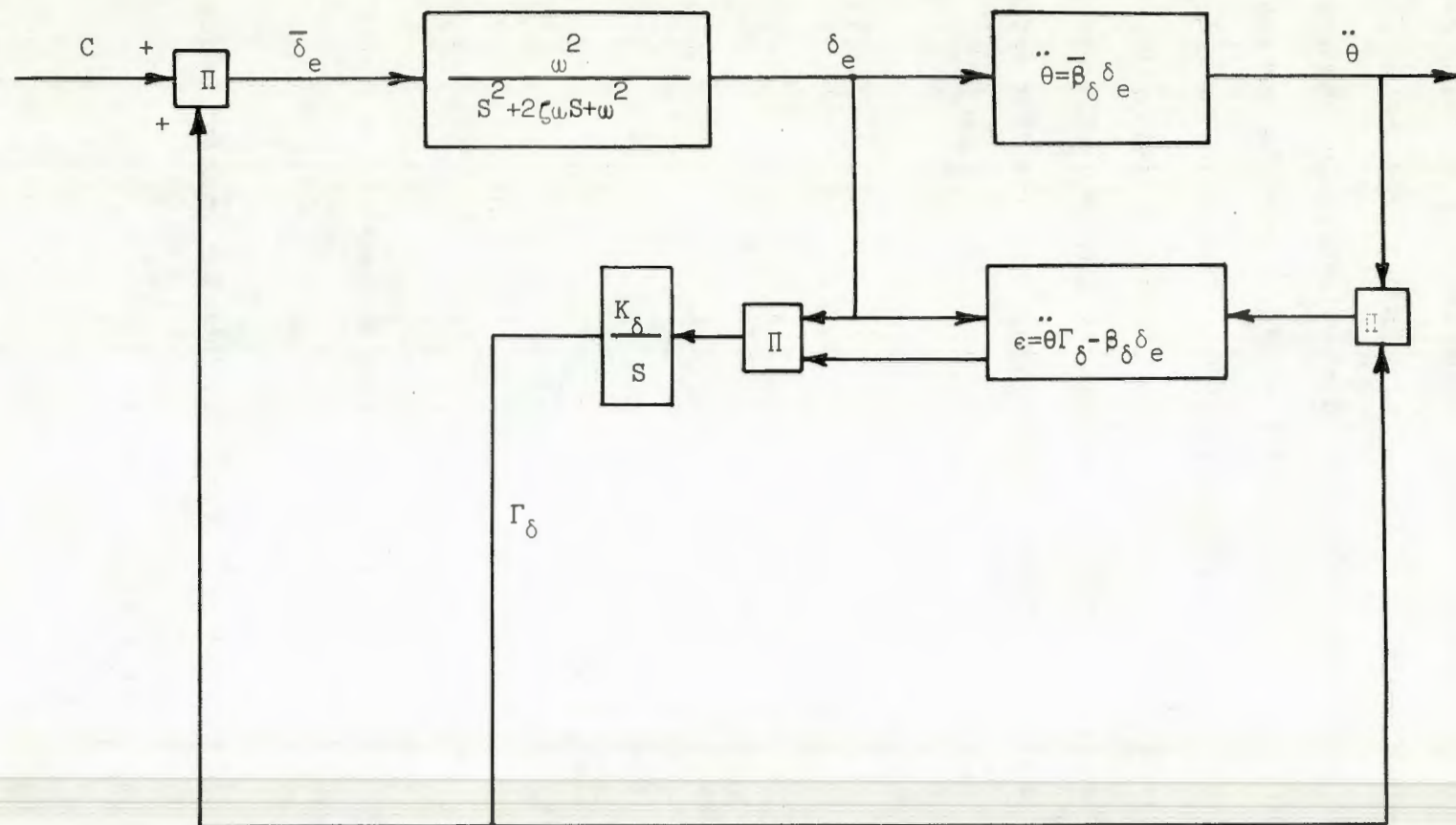


FIGURE 25. BLOCK DIAGRAM FOR MODIFIED $\Gamma_\delta C$ -SYSTEM

Since $\bar{\beta}_\delta$ is always negative, the gradient is therefore also always negative and thus v and ϵ approach zero as time proceeds. The ideal value of the variable gain Γ_δ may also be calculated from the error relationship:

$$\epsilon = \ddot{\theta}\Gamma_\delta - \beta_\delta \delta_e$$

$$\epsilon = [\bar{\beta}_\delta \Gamma_\delta - \beta_\delta] \delta_e$$

$$\therefore \Gamma_\delta^* = \frac{\beta_\delta}{\bar{\beta}_\delta} \text{ for } \epsilon \equiv 0.$$

The new simplified $\Gamma_\delta C$ -system is therefore adaptive since the variable gain will approach its ideal value as the error approaches zero and it seems to be a reasonable system to eliminate the parasitic oscillations of the previous $\Gamma_\delta C$ -controller.

A short study of the stability of the modified $\Gamma_\delta C$ -controller will show whether or not limit cycle oscillations should be expected to occur in the system. The set of equations which describe the controller may be combined to yield

$$\frac{d\Gamma_\delta}{dt} = K_\delta \delta_e^2 (\bar{\beta}_\delta \Gamma_\delta - \beta_\delta)$$

$$\text{and } \ddot{\delta}_e + 2\zeta\omega\dot{\delta}_e + \omega^2\delta_e = \omega^2\Gamma_\delta C.$$

If C is set equal to C_0 and the steady state operation is observed, then $\dot{\Gamma}_\delta = 0$, $\dot{\delta}_e = 0$, and $\ddot{\delta}_e = 0$. Therefore,

$$0 = K_\delta \delta_e^2 (\bar{\beta}_\delta \Gamma_{\delta_0} + \beta_\delta)$$

and $\delta_{e_0} = C_0 \Gamma_{\delta_0}$. The steady state values of Γ_δ and δ_e may be calculated to give

$$\Gamma_{\delta_0} = \frac{\beta_\delta}{\bar{\beta}_\delta} \quad \text{and} \quad \delta_{e_0} = C_0 \frac{\beta_\delta}{\bar{\beta}_\delta}.$$

Now, substituting the small perturbation relationships

$$\delta_e = \delta_{e_0} + \hat{\delta}_e$$

$$\Gamma_\delta = \Gamma_{\delta_0} + \hat{\Gamma}_\delta$$

into the combined controller equations yields

$$\frac{d\hat{\Gamma}_\delta}{dt} = K_\delta (\delta_{e_o} + \hat{\delta}_e)^2 [\bar{\beta}_\delta (\Gamma_{\delta_o} + \hat{\Gamma}_\delta) - \beta_\delta]$$

$$\hat{\delta}_e + 2\zeta\omega\dot{\hat{\delta}}_e + \omega^2(\delta_{e_o} + \hat{\delta}_e) = \omega^2 C_o (\Gamma_{\delta_o} + \hat{\Gamma}_\delta).$$

If the previous steady state relationships are used, the equations reduce to

$$\frac{d\hat{\Gamma}_\delta}{dt} = K_\delta \delta_{e_o}^2 \bar{\beta}_\delta \hat{\Gamma}_\delta$$

$$\hat{\delta}_e + 2\zeta\omega\dot{\hat{\delta}}_e + \omega^2\hat{\delta}_e = \omega^2\hat{\Gamma}_\delta$$

which results in the following characteristic equation,

$$(\lambda - K_\delta \delta_{e_o}^2 \bar{\beta}_\delta)(\lambda^2 + 2\zeta\omega\lambda + \omega^2) = 0.$$

The system has three roots and since $\bar{\beta}_\delta$ is always negative, it is obvious that all three roots have negative real parts, which indicates that the system is always stable. Any disturbance to the system will die out and limit cycles cannot occur.

Observing the perturbed $\Gamma_\delta C$ -system shows that the phase shift can never cross -180 degrees which also indicates limit cycles cannot occur. These observations will be verified by analog simulation of the controller. The perturbed system equations are

$$C = C_o$$

$$\Gamma_\delta = \frac{\beta_\delta}{\bar{\beta}_\delta} + \gamma$$

$$\epsilon = \ddot{\Theta}\Gamma_\delta - \beta_\delta \delta_e,$$

where γ and ϵ drive the system until $\gamma = 0$, $\epsilon = 0$, and $\Gamma_\delta = \Gamma_\delta^*$. It is also known that

$$\bar{\delta}_e = \Gamma_\delta C_o = \frac{\beta_\delta}{\bar{\beta}_\delta} C_o + \gamma C_o$$

and $\delta_e = \delta_{e_o} + \hat{\delta}_e$ where $\delta_{e_o} = \frac{\beta_\delta}{\bar{\beta}_\delta} C_o$. A relationship for pitch acceleration may be derived from the plant equation

$$\ddot{\theta} = \bar{\beta}_\delta \delta_e = \bar{\beta}_\delta C_o \frac{\beta_\delta}{\bar{\beta}_\delta} + \bar{\beta}_\delta \hat{\delta}_e = C_o \beta_\delta + \bar{\beta}_\delta \hat{\delta}_e$$

and introduced into the error equation to yield

$$\epsilon = \left(\frac{\beta_\delta}{\bar{\beta}_\delta} + \gamma \right) (C_o \beta_\delta + \bar{\beta}_\delta \hat{\delta}_e) - \beta_\delta \left(\frac{\beta_\delta}{\bar{\beta}_\delta} C_o + \hat{\delta}_e \right)$$

$$\epsilon = \gamma \beta_\delta C_o + \beta_\delta \hat{\delta}_e \gamma$$

$$\epsilon = \gamma \beta_\delta C_o$$

Substituting the error relationship into the equation for the variable gain results in the following derivation:

$$\frac{d\Gamma_\delta}{dt} = \frac{d}{dt} \left[\frac{\beta_\delta}{\bar{\beta}_\delta} + \gamma \right] = \frac{d\gamma}{dt} = K_\delta (\delta_{e_o} + \hat{\delta}_e) \epsilon$$

$$\frac{d\gamma}{dt} = K_\delta \frac{\beta_\delta C_o}{\bar{\beta}_\delta} \gamma \beta_\delta C_o$$

and introducing the relay,

$$\frac{d\gamma}{dt} = K_\delta \frac{\beta_\delta C_o}{\bar{\beta}_\delta} \operatorname{sgn} (\gamma \beta_\delta C_o).$$

This equation plus a relationship for the second order servo

$$\hat{\delta}_e + 2\zeta\omega\hat{\delta}_e + \omega^2\delta_e = \omega^2\gamma C_o$$

describes the perturbed modified $\Gamma_\delta C$ -system shown in Figure 26. This figure shows that in the perturbed control loop, the maximum possible phase shift is -90 degrees. Therefore, the phase shift cannot pass through -180 degrees and limit cycles cannot occur.

The $\Gamma_\delta C$ -controller was shown to exhibit limit cycles in Figures 7 and 8. With the same parameters for the second order servo and variable gain, the modified $\Gamma_\delta C$ -controller is shown in Figure 27. The system

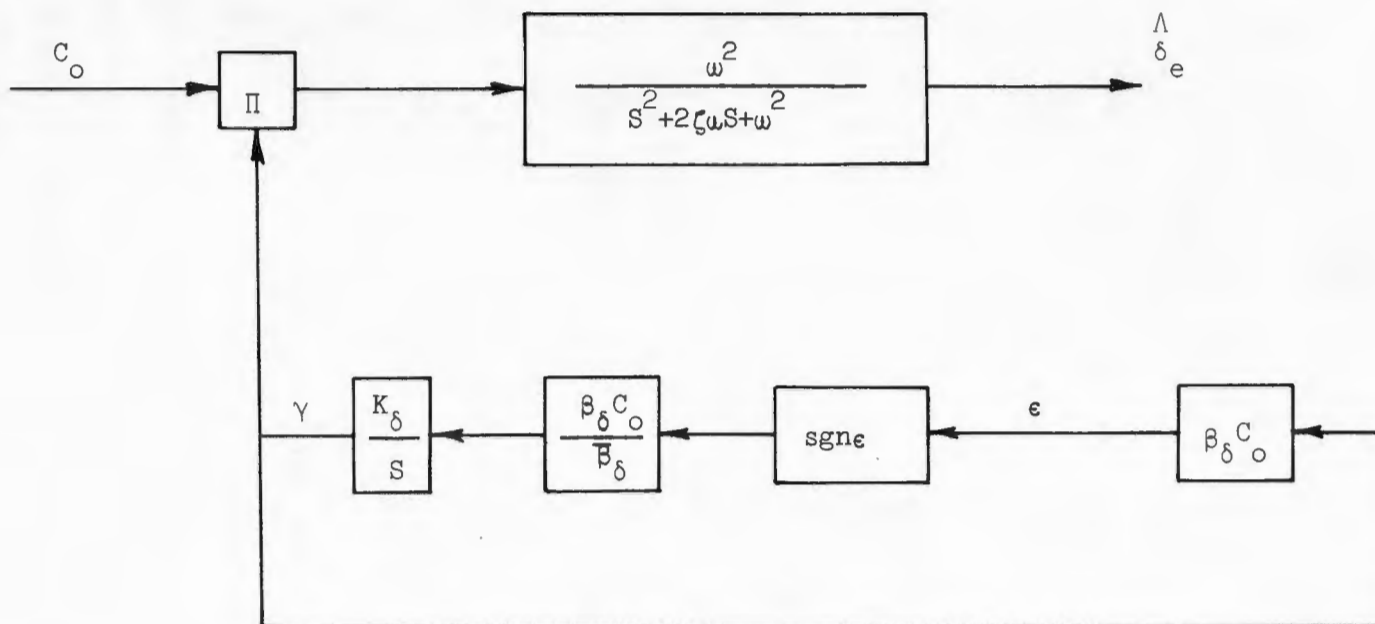


FIGURE 26. BLOCK DIAGRAM FOR PERTURBED MODIFIED Γ_δ C-SYSTEM

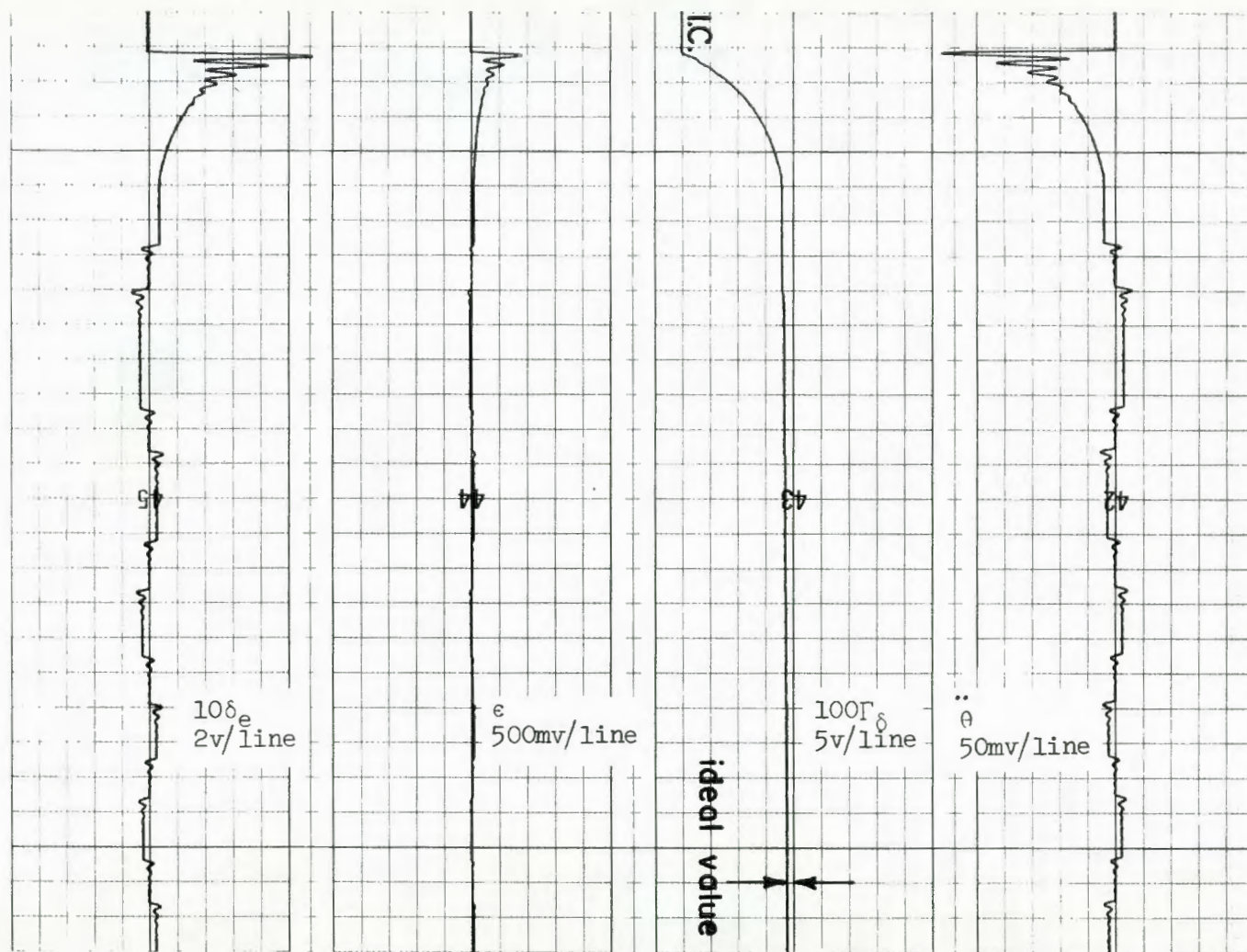


FIGURE 27. ANALOG TRACE FOR MODIFIED Γ_δ C-SYSTEM, NO LIMIT CYCLES

does not exhibit limit cycle oscillations as the variable gain approaches its ideal value and the error approaches zero. A more detailed study of the control systems will be contained in Chapter VII for the complete nonvarying- C^* adaptive control system.

VI. THE MODIFIED NONVARYING-C* ADAPTIVE CONTROLLER

The simplified controller studied in the previous chapter may be expanded to the complete modified nonvarying-C* adaptive control system. The system must have the same fundamental aircraft equation as the adaptive control system studied in Chapter II,

$$\ddot{\theta} = \bar{\beta}_q \dot{\theta} + \bar{\beta}_n n + \bar{\beta}_\delta \delta_e.$$

The other governing equations for the controller were developed by trial and error using the information available from the simplified system and the Gradient Technique to insure that the system was adaptive. The error equation was computed for each configuration and from this relationship, the gradient could be set up. By choosing desirable values for the variable gains, the sign of the gradient could be calculated, and if the gradient was negative for all time, then the system error would approach zero. Using this method, the equations for the modified nonvarying-C* adaptive controller were calculated:

$$\epsilon = \Gamma_\delta [\ddot{\theta} + \beta_\delta (\Gamma_n n + \Gamma_q \dot{\theta}) - (\beta_q \dot{\theta} + \beta_n n)] - \beta_\delta \delta_e$$

$$\frac{d\Gamma_\delta}{dt} = K_\delta \delta \operatorname{sgn} \epsilon$$

$$\frac{d\Gamma_n}{dt} = K_n \Gamma_\delta n \operatorname{sgn} \epsilon$$

$$\frac{d\Gamma_q}{dt} = K_q \Gamma_\delta \dot{\theta} \operatorname{sgn} \epsilon$$

$$\bar{\delta}_e = \Gamma_\delta [C + \Gamma_n n + \Gamma_q \dot{\theta}]$$

$$\ddot{\delta}_e + 2\zeta\omega\dot{\delta}_e + \omega^2\delta_e = \omega^2\bar{\delta}_e.$$

The block diagram for this system is shown on Figure 28. Rearranging the error equation,

$$\begin{aligned}\epsilon = & [\Gamma_\delta \bar{\beta}_\delta - \beta_\delta] \delta_e + \Gamma_\delta [\bar{\beta}_q + \beta_\delta \Gamma_q - \beta_q] \dot{\theta} \\ & + \Gamma_\delta [\bar{\beta}_n + \beta_\delta \Gamma_n - \beta_n] n ,\end{aligned}$$

allows the calculation of the ideal values of the variable gains:

for $\epsilon \equiv 0$

$$\begin{aligned}\Gamma_\delta^* &= \frac{\beta_\delta}{\bar{\beta}_\delta} \\ \Gamma_q^* &= \frac{\beta_q - \bar{\beta}_q}{\beta_\delta} \\ \Gamma_n^* &= \frac{\beta_n - \bar{\beta}_n}{\beta_\delta} .\end{aligned}$$

From the previous error relationship, also consider,

$$\begin{aligned}\frac{dv}{dt} = & \beta_\delta \left\{ \frac{1}{K_\delta} [\Gamma_\delta \bar{\beta}_\delta - \beta_\delta] \frac{d\Gamma_\delta}{dt} + \frac{1}{K_q} [\bar{\beta}_q + \beta_\delta \Gamma_q - \beta_q] \frac{d\Gamma_q}{dt} \right. \\ & \left. + \frac{1}{K_n} [\bar{\beta}_n + \beta_\delta \Gamma_n - \beta_n] \frac{d\Gamma_n}{dt} \right\} .\end{aligned}$$

Choosing

$$\frac{d\Gamma_\delta}{dt} = K_\delta \delta_e G \quad ; \quad \frac{d\Gamma_q}{dt} = K_q \Gamma_\delta \dot{\theta} G \quad ; \quad \frac{d\Gamma_n}{dt} = K_n \Gamma_\delta n G$$

yields $\frac{dv}{dt} = \beta_\delta \epsilon G$ which is negative; therefore ϵ approaches zero. From the fundamental aircraft equation and the relationship for δ_e (neglecting the servo) it may be shown that

$$\ddot{\theta} = \bar{\beta}_q \dot{\theta} + \bar{\beta}_n n + \bar{\beta}_\delta [\Gamma_\delta (C + \Gamma_q \dot{\theta} + \Gamma_n n)] .$$

If the ideal values of the variable gains are used in the previous equation,

$$\ddot{\theta} = \bar{\beta}_q \dot{\theta} + \bar{\beta}_n n + \bar{\beta}_\delta \frac{\beta_\delta}{\bar{\beta}_\delta} \left[C + \frac{\beta_q - \bar{\beta}_q}{\beta_\delta} \dot{\theta} + \frac{\beta_n - \bar{\beta}_n}{\beta_\delta} n \right] ,$$

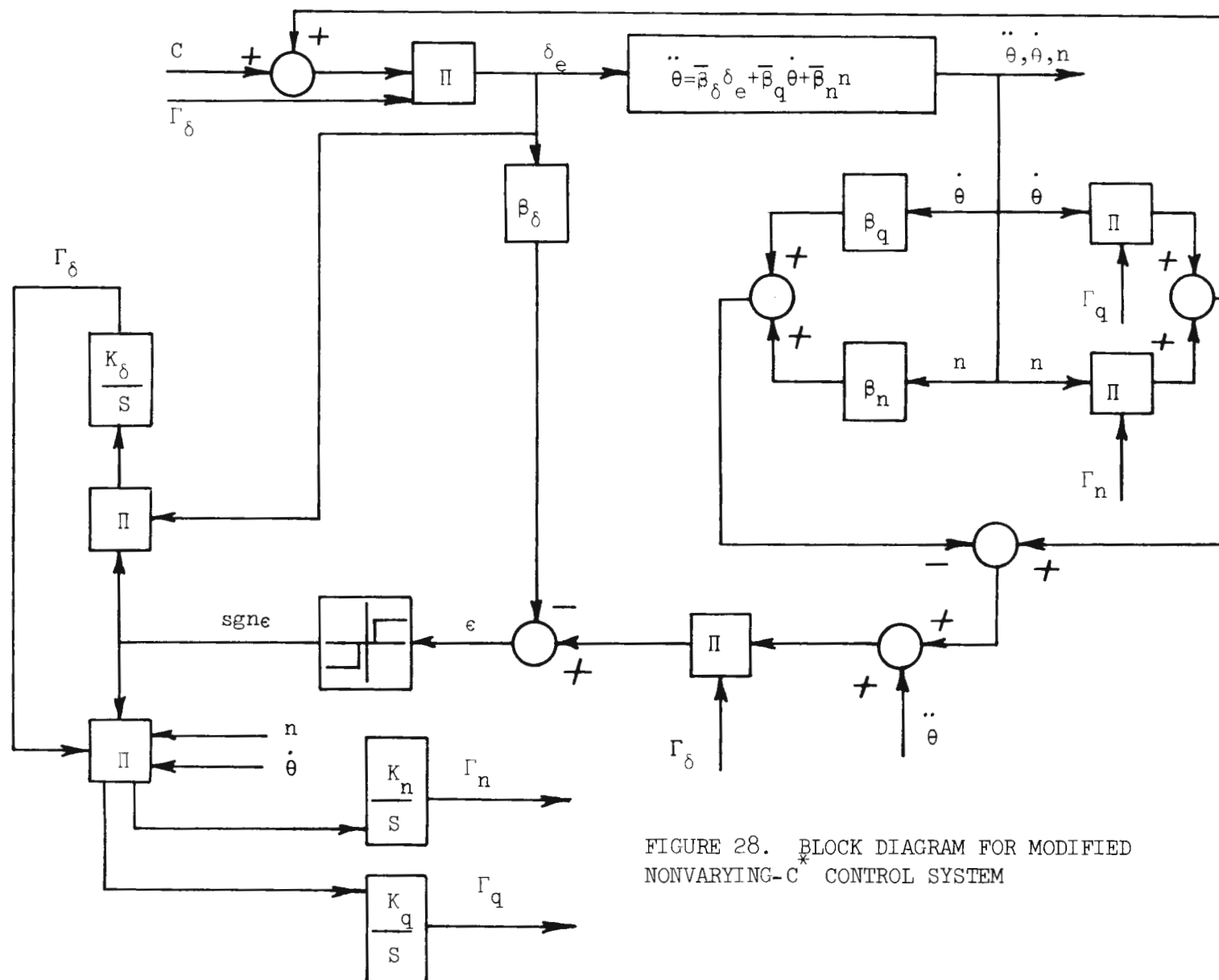


FIGURE 28. BLOCK DIAGRAM FOR MODIFIED
NONVARYING- C CONTROL SYSTEM

then $\ddot{\theta} = \beta_q \dot{\theta} + \beta_n n + \beta_\delta C$, which is the C*-criterion as developed in Chapter II. The system has thus been proven to be adaptive and when the error is zero the aircraft behaves as if the fundamental aircraft equation were exactly that of the criterion. A detailed comparison of the two nonvarying-C* adaptive controllers will be shown in the next chapter.

VII. ANALOG STUDY OF TWO NONVARYING-C* ADAPTIVE CONTROL SYSTEMS

The analog diagram used for the simulation of the original C*-controller was shown in Figure 14. The analog diagram for the modified C*-controller is shown in Figure 29. The potentiometer settings for the aircraft and controller parameters for these analog diagrams are listed on Table I. All analog simulation was done on the CI 5000 analog computer.

The original controller was studied in Chapter III for a flight condition of Mach 2 at 50,000 feet. Analog traces confirm the values of the variable gains listed on Table II without the complications introduced by the servo or the actuator. Traces are also shown for the control system with the actuator and with both the actuator and the servo in the system, resulting in limit cycles. Similar studies were made at flight conditions of Mach .9 at sea level and Mach .2 at sea level with comparable results. The flight parameters for the simulation were taken from F-4 data which appears on Table I.

The modified controller was also studied at the same three flight conditions. The aircraft parameters were for the same aircraft and also appear on Table I. The ideal values for the variable gains of the modified controller are shown on Table II. The traces for the free aircraft without and with the actuator will be the same as shown in Figure 15 and 16 respectively since the fundamental aircraft equations are the same for both controllers. The modified controller, with actuator and feedback, for flight condition Mach 2 at 50,000 feet is shown in Figure 30. Note that the values of the variable gains approach their ideal values as listed in Table II even though the complication

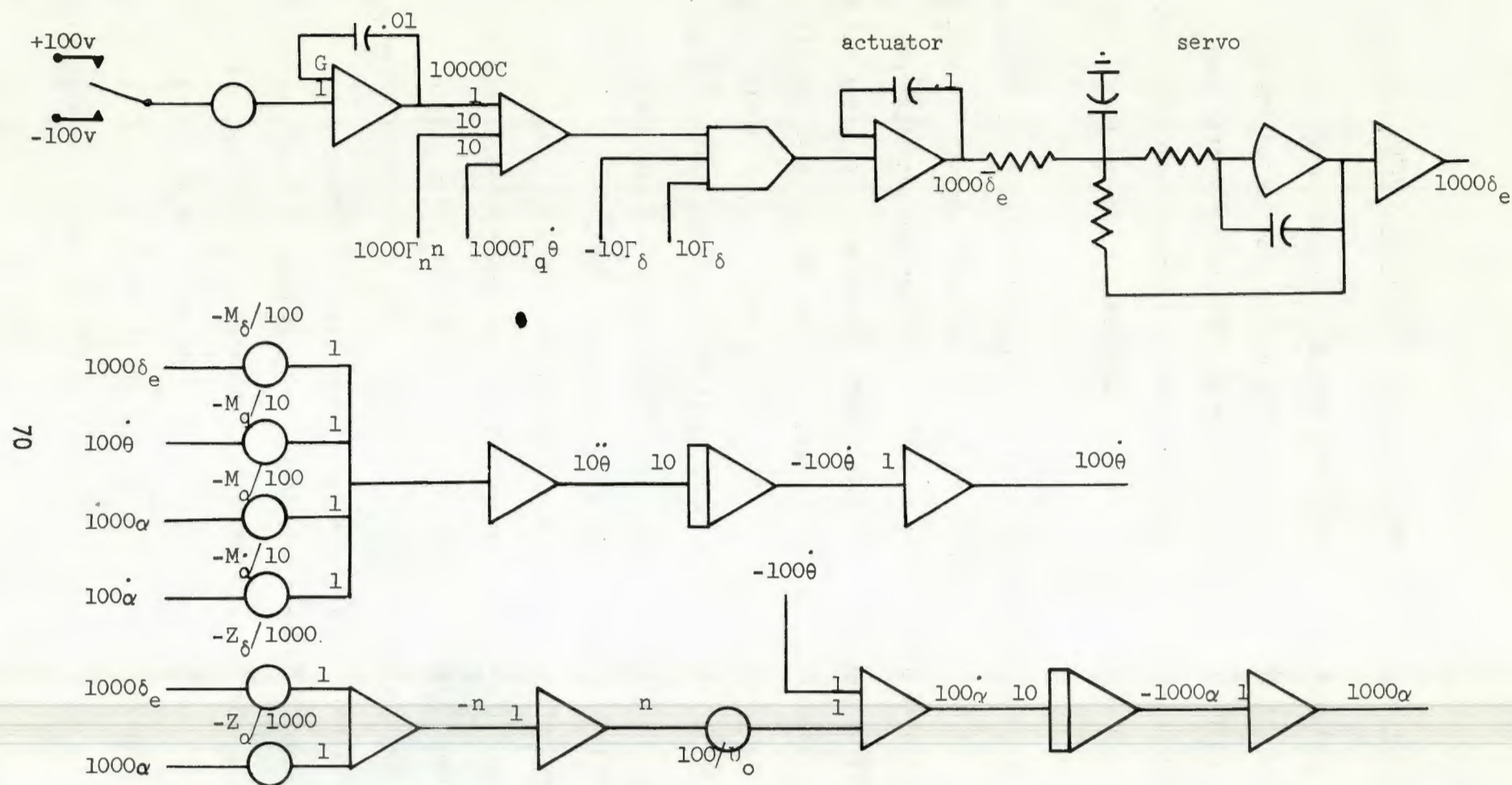


FIGURE 29. ANALOG DIAGRAM FOR MODIFIED NONVARYING- C^* CONTROL SYSTEM

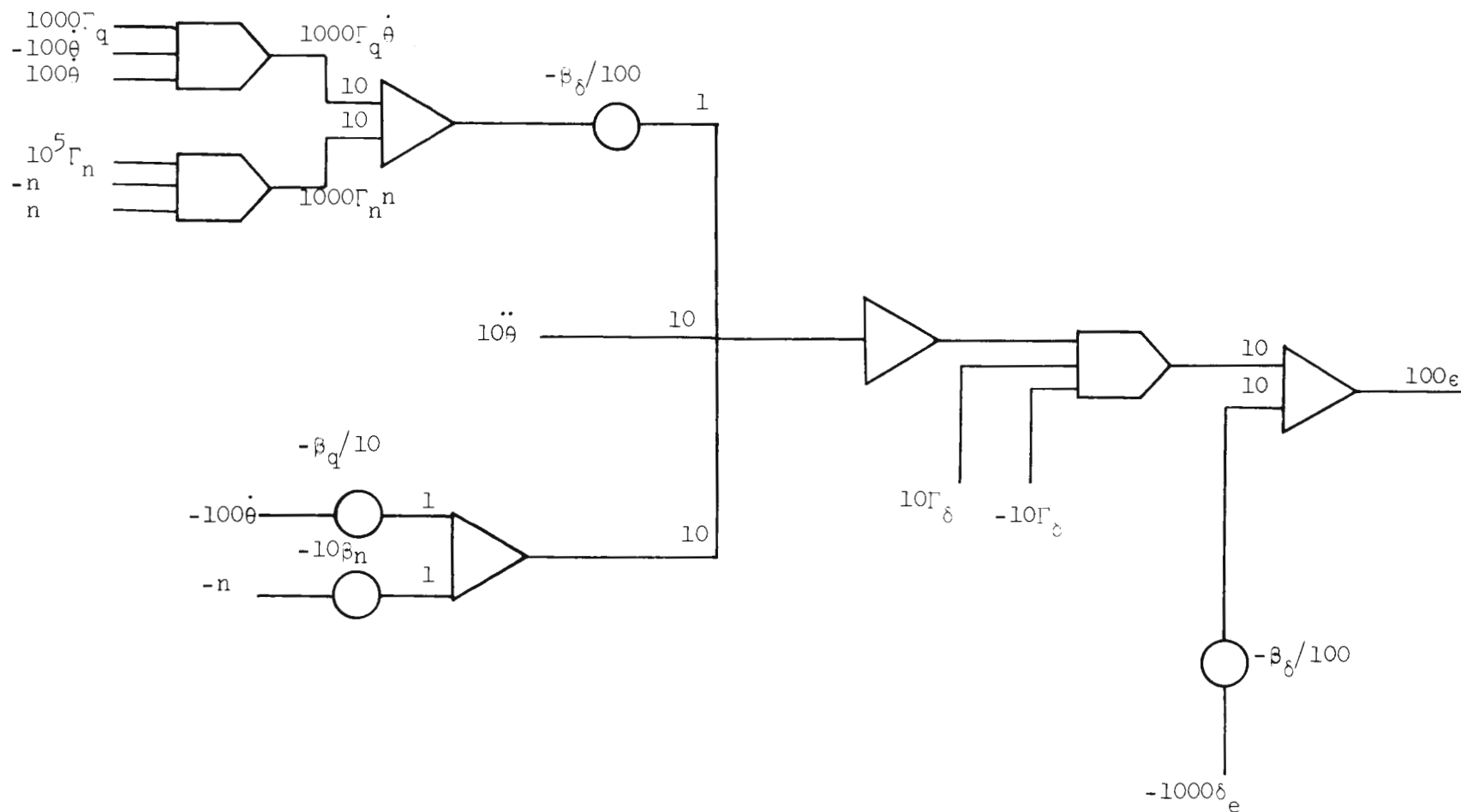


FIGURE 29. ANALOG DIAGRAM FOR MODIFIED NONVARYING- C^* CONTROL SYSTEM

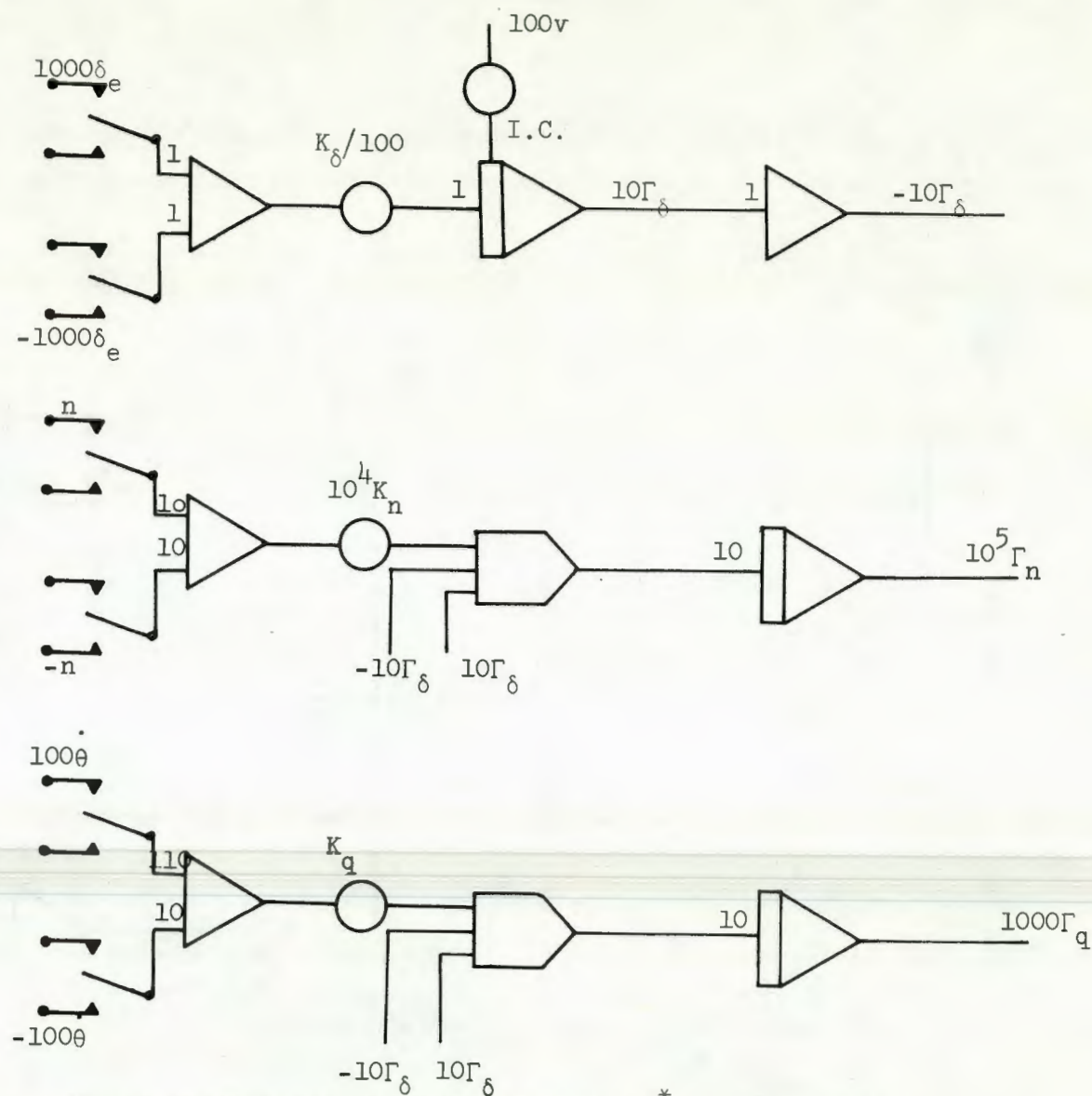


FIGURE 29. ANALOG DIAGRAM FOR MODIFIED NONVARYING- C^* CONTROL SYSTEM

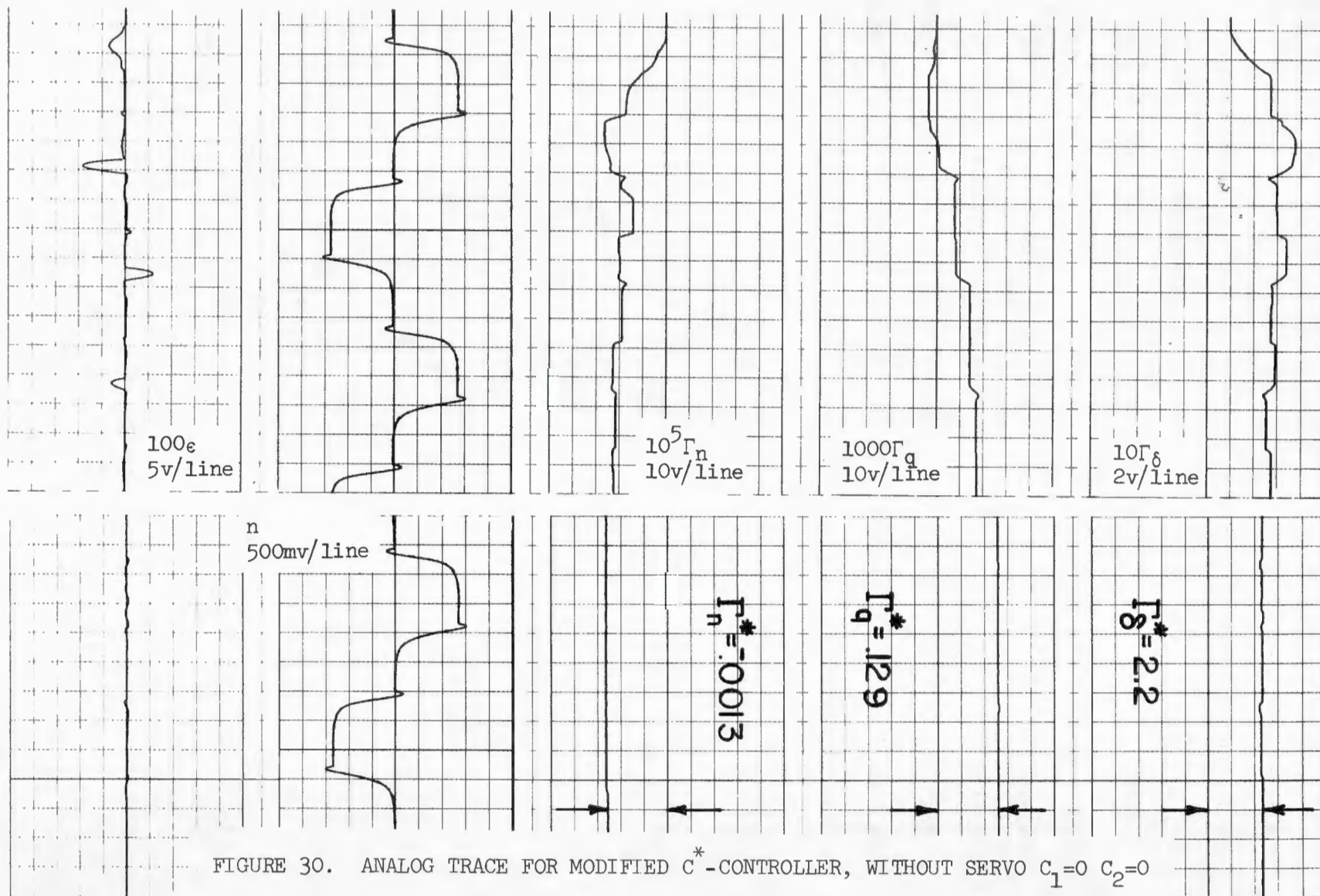


FIGURE 30. ANALOG TRACE FOR MODIFIED C^* -CONTROLLER, WITHOUT SERVO $C_1=0$ $C_2=0$

introduced by the actuator is present. This results from the fact that the actuator, like the second order servo, is no longer in the perturbed system control loop and does not effect the values attained by the variable gains. Figures 31, 32, and 33 show the modified controller with the actuator and the second order servo at flight conditions of Mach 2 at 50,000 feet, Mach .2 at sea level, and Mach .9 at sea level respectively. Limit cycle oscillations did not appear at any flight condition, further the controller was completely stable at all flight conditions studied. The modified nonvarying-C* adaptive control system was thus shown to be practical and free of limit cycle oscillations by analog simulation.

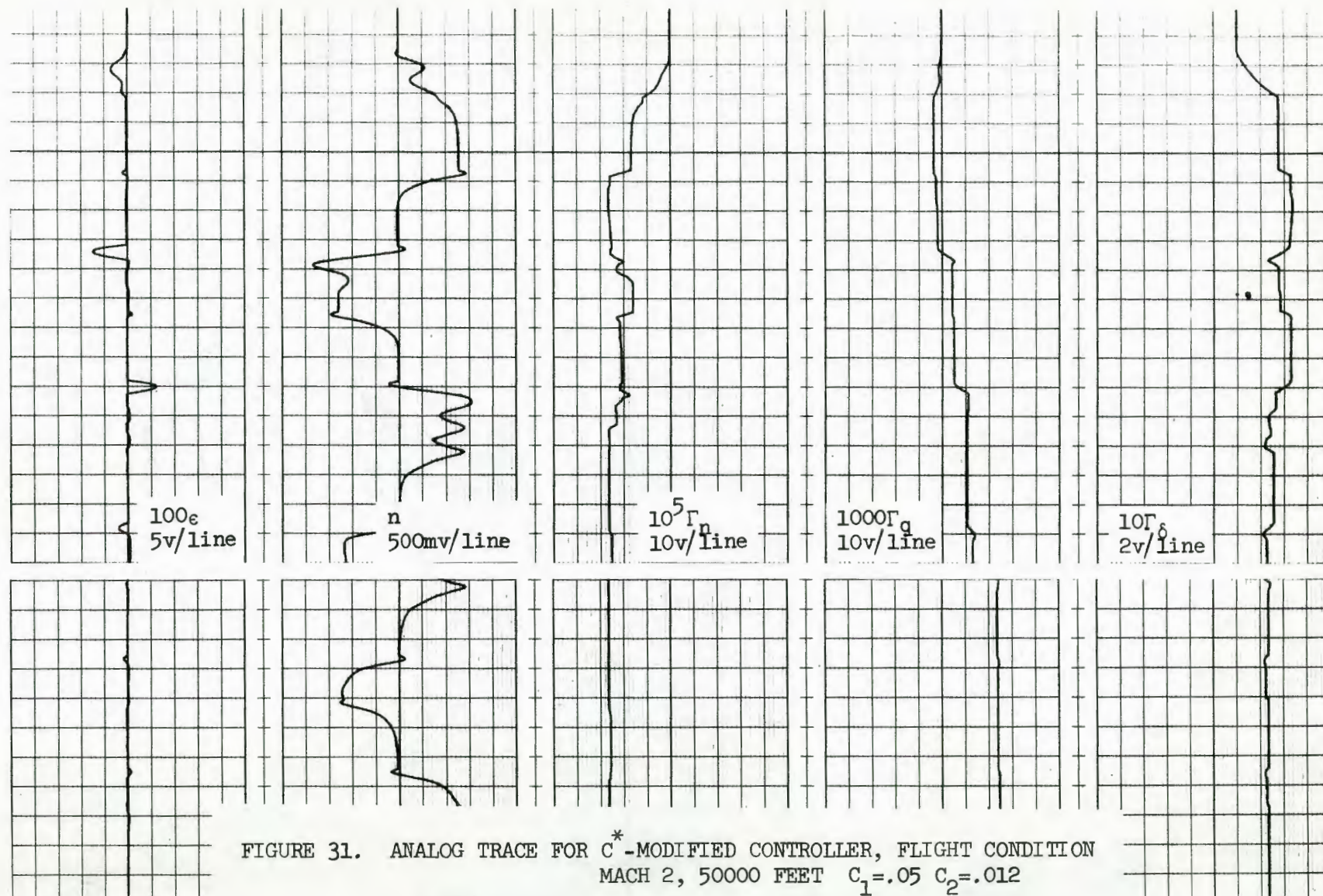


FIGURE 31. ANALOG TRACE FOR C^* -MODIFIED CONTROLLER, FLIGHT CONDITION
MACH 2, 50000 FEET $C_1=.05$ $C_2=.012$

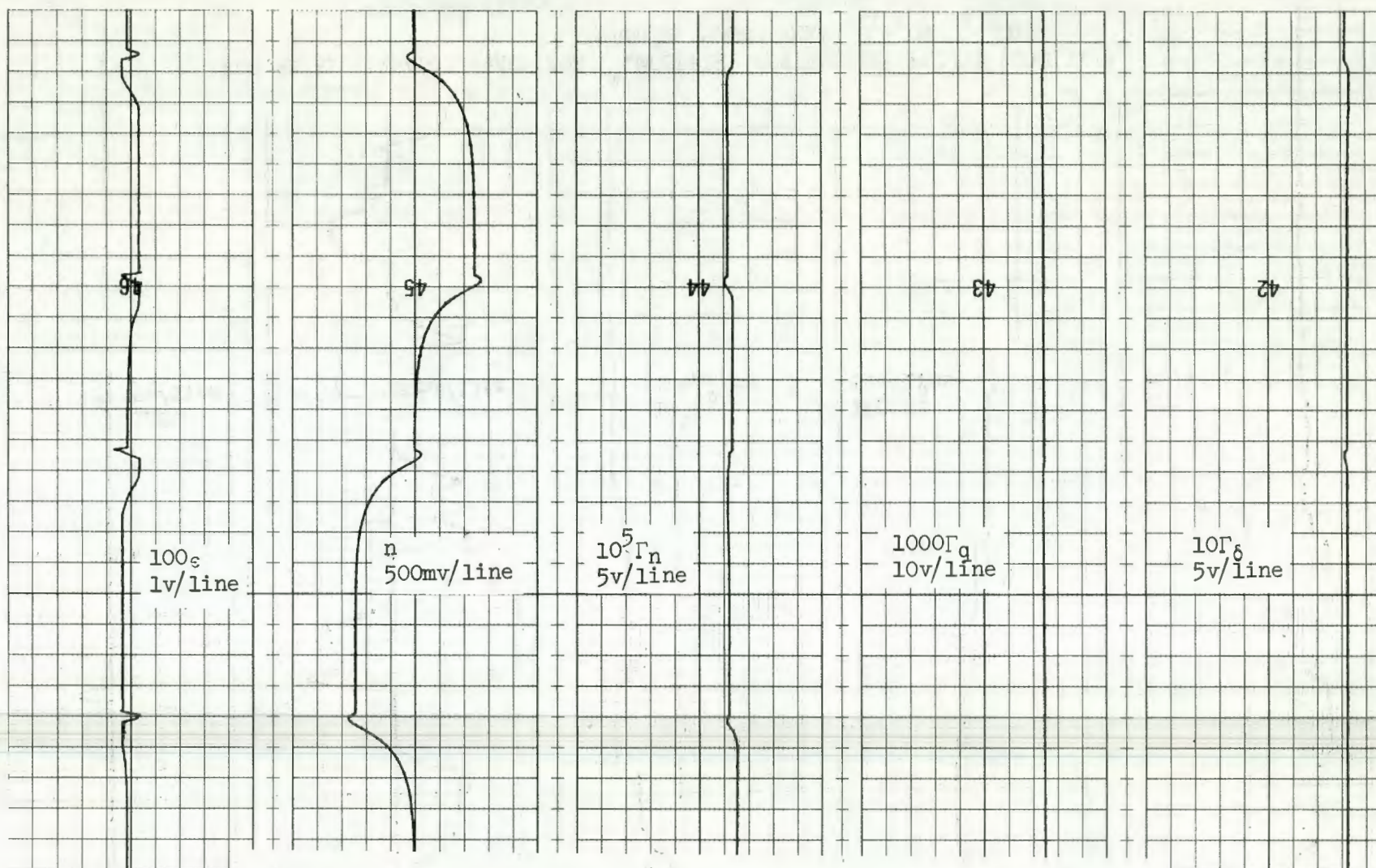


FIGURE 32. ANALOG TRACE FOR C*-MODIFIED CONTROLLER, FLIGHT CONDITION
MACH .2, SEA LEVEL $C_1=.05$ $C_2=.012$

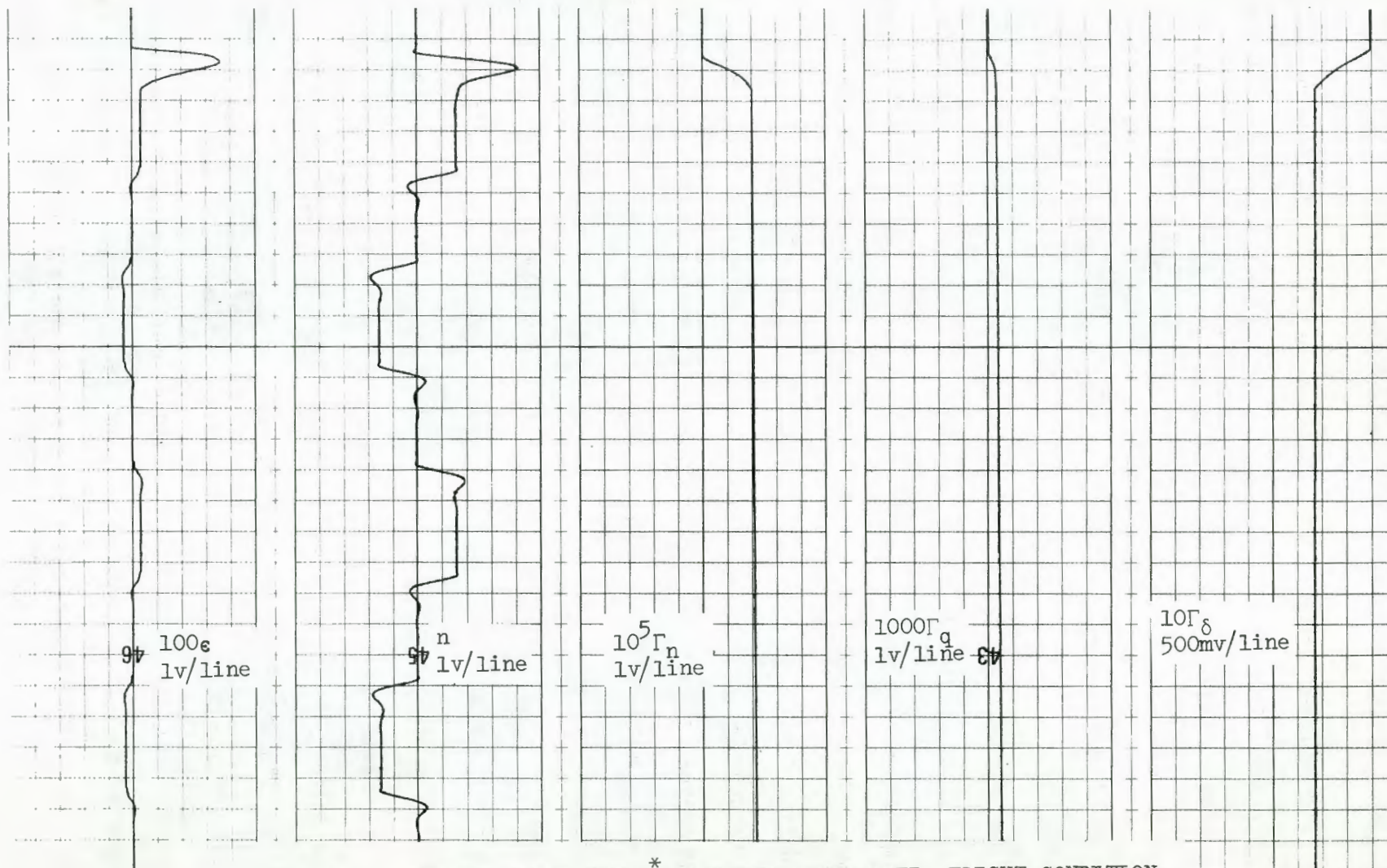


FIGURE 33. ANALOG TRACE FOR C^* -MODIFIED CONTROLLER, FLIGHT CONDITION
MACH .9, SEA LEVEL $C_1=.05$ $C_2=.012$

VIII. CONCLUSIONS AND RECOMMENDATIONS

The original nonvarying-C* adaptive controller had inherent limit cycle oscillations in the system. The two fixes for the problem were to increase the deadband on the relay and to modify the system to prevent the phase shift from passing through -180 degrees, both of which eliminated the oscillations. Modification of the controller, being the most practical approach, was studied thoroughly.

A modified nonvarying-C* adaptive controller was designed and shown to be practical by analog simulation. An analytic study of the stability of the modified system together with a study of the perturbed control loop resulted in proof that limit cycles could not occur in the modified controller even under large input commands. The complications introduced by the actuator and the servo in the modified controller did not prevent the variable gains from approaching their ideal values as in the original controller, since the actuator and servo are not in the perturbed control loop of the modified system.

Future study of the modified controller might include: an investigation of optimal gain constants, simplification of the modified system by further analog study, effects of gust inputs, a study of signal noise, a study of elevator hysteresis, and a control system flight simulation. The gains or constants K_δ , K_q , and K_n determine how fast or slow the integrations resulting in Γ_δ , Γ_q , and Γ_n take place. An optimal value for each of these constants will result in a rapid approach of the variable gains to their ideal values without a large amount of initial overshoot at all flight conditions. The quicker the variable gains approach their ideal values for a specific flight

condition, the quicker the system error becomes zero and the aircraft will be flying as if its governing equation were exactly that of the C*-criterion.

The modified controller could probably be simplified from its present configuration. A more intensive analog study of the system would reveal whether or not the modified controller could be simplified and retain comparable adaptive characteristics. Figure 28 shows that Γ_δ is a common multiplication factor in the calculation of both Γ_q and Γ_n . By adjusting the constants K_q and K_n , this multiplication could probably be eliminated. Other simplifications might result from continued analog simulation resulting in a more compact controller with acceptable characteristics.

A complete study of signal noise in the system, elevator hysteresis, and the effects of gust inputs should be made on the modified controller. These complications are all present in a real physical control system and should be studied by simulation on the analog computer. A step gust input and signal noise in the mechanical linkages could be simulated and summed with the angle of attack signal to give total angle of attack; whereas, a model for elevator hysteresis could be patched in series with the actuator and series servo to give the elevator signal. Previous control systems have been shown to operate perfectly without the above conditions, but to fail as an operational adaptive controller with the introduction of one or more of these complications.

After the system appears to be performing satisfactorily by the analog simulation, a flight simulation could be performed to determine pilot opinion of the controller. The Naval Postgraduate School variable stability flight simulator is capable of patching directly to the hybrid

computer's analog board. By so doing, the flying qualities of the aircraft with the modified controller could be studied at different flight conditions simply by resetting the potentiometers or by using a digital program to set the potentiometers for each flight condition or for each different aircraft under study. Since the Naval Postgraduate School has many naval aviators, the flight simulator could be flown by a number of pilots and rated to determine handling qualities of the aircraft with the modified controller.

BIBLIOGRAPHY

1. Rang, E. R., "A Nonvarying-C* Control Scheme for Aircraft," Naval Postgraduate School Technical Report, June 1969. (To be published.)
2. Shipley, P. P., Engle, A. G., Jr., and Hung, J. W., "Self-Adaptive Control by Multivariable Parameter Identification," AFFDL-TR-65-90, August 1965.
3. Elgerd, O. I., Control System Theory, New York: McGraw-Hill Book Co., Inc., 1967.
4. Gibson, J. E., Nonlinear Automatic Control, New York: McGraw-Hill Book Co., Inc., 1963.
5. Abramson, H. N., Liebowitz, H., Crowley, J. M., and Juhasz, S., Applied Mechanics Surveys, Washington, D.C.: Spartan Books, 1966.
6. Rang, E. R., "Adaptive Controllers Derived by Stability Considerations," Honeywell Report MH-MPG 1529-TR9, 15 March 1962.
7. Thaler, G. J., and Brown, R. G., Analysis and Design of Feedback Control Systems, New York: McGraw-Hill Book Co., Inc., 1960.
8. Thaler, G. J., and Pastel, M. P., Analysis and Design of Nonlinear Feedback Control Systems, New York: McGraw-Hill Book Co., Inc., 1962.

INITIAL DISTRIBUTION LIST

	No. Copies
1. Defense Documentation Center Cameron Station Alexandria, Virginia 22314	20
2. Library Naval Postgraduate School Monterey, California 93940	2
3. Chairman, Department of Aeronautics Naval Postgraduate School Monterey, California 93940	1
4. Commander, Naval Air Systems Command Navy Department Washington, D. C. 20360	1
5. Mr. Robert F. Lawson Office of Naval Research 1030 East Green Street Pasadena, California 91109	1
6. Mr. E. M. Elliott Boeing Company (4C-79) P. O. Box 3733 Seattle, Washington 98124	1
7. Mr. Dennis Cannon Department of Aerospace Engineering University of Kansas Lawrence, Kansas 66645	1
8. Professor Edward R. Rang Department of Aeronautics Naval Postgraduate School Monterey, California 93940	1
9. LTJG Larry S. Wisler, USN 1320 West 27 G-48 Topeka, Kansas 66611	1

DOCUMENT CONTROL DATA - R & D

(Security classification of title, body of abstract and indexing annotation must be entered when the overall report is classified)

1. ORIGINATING ACTIVITY (Corporate author) Naval Postgraduate School Monterey, California 93940		2a. REPORT SECURITY CLASSIFICATION Unclassified	
		2b. GROUP	
3. REPORT TITLE An Investigation of Oscillations in an Adaptive Aircraft Control System Under Large Input Commands			
4. DESCRIPTIVE NOTES (Type of report and inclusive dates) Master's Thesis; June 1969			
5. AUTHOR(S) (First name, middle initial, last name) Larry Smith Wisler			
6. REPORT DATE June 1969		7a. TOTAL NO. OF PAGES 81	7b. NO. OF REFS 8
8a. CONTRACT OR GRANT NO.		9a. ORIGINATOR'S REPORT NUMBER(S)	
b. PROJECT NO.			
c.		9b. OTHER REPORT NO(S) (Any other numbers that may be assigned this report)	
d.			
10. DISTRIBUTION STATEMENT Distribution of this document is unlimited.			
11. SUPPLEMENTARY NOTES		12. SPONSORING MILITARY ACTIVITY Naval Postgraduate School Monterey, California 93940	

13. ABSTRACT

An adaptive control scheme for aircraft was studied to find the cause of limit cycles which occurred under large input commands and to find a method for eliminating the oscillations. The complexity of the system equations dictated that all analytical studies be performed on simplified versions of the adaptive control scheme. After exhaustive analysis of the cause of limit cycles in the simplified systems and an investigation of possible fixes for this problem, it was decided that the oscillations were an inherent feature of the control scheme resulting from the servo and actuator lags.

A second adaptive control scheme was thus developed which obtained more feedback information downstream of the aircraft actuator and series servo. A comparison of the two adaptive systems was made under similar flight conditions for the F-4 aircraft and the modified adaptive controller was shown to be practical and free of limit cycle oscillations by analog simulation.

14

KEY WORDS

LINK A

LINK B

LINK C

ROLE

WT

ROLE

WT

ROLE

WT

Automatic control
Hybrid computer
Adaptive controller
Limit cycles
Aircraft control
Nonlinear oscillations



thesW663
An investigation of oscillations in an a



3 2768 001 90006 1
DUDLEY KNOX LIBRARY